IACMI/0001-2017/3.4

Thermoplastic Composites Parts Manufacturing Enabling High Volumes, Low Cost, Reduced Weight with Design Flexibility – Phase 1

Authors:
Lee Silverman
Michael Bogdanor
Robert Davies
Jacob Dickinson

Date Published

April 24, 2018

The Institute for iacmi Advanced Composites Manufacturing Innovation
THE COMPOSITES INSTITUTE

U.S. DEPARTMENT OF ENERGY

DOCUMENT AVAILABILITY

Reports produced after January 1, 1996, are generally available free via US Department of Energy (DOE) SciTech Connect.

Website http://www.osti.gov/scitech/

Reports produced before January 1, 1996, may be purchased by members of the public from the following source:

National Technical Information Service
5285 Port Royal Road
Springfield, VA 22161
Telephone 703-605-6000 (1-800-553-6847)
TDD 703-487-4639
Fax 703-605-6900
E-mail info@ntis.gov
Website http://www.ntis.gov/help/ordermethods.aspx

Reports are available to DOE employees, DOE contractors, Energy Technology Data Exchange representatives, and International Nuclear Information System representatives from the following source:

Office of Scientific and Technical Information
PO Box 62
Oak Ridge, TN 37831
Telephone 865-576-8401
Fax 865-576-5728
E-mail reports@osti.gov
Website http://www.osti.gov/contact.html

Disclaimer: "The information, data, or work presented herein was funded in part by an agency of the United States Government. Neither the United States Government nor any agency thereof, nor any of their employees, makes any warranty, express or implied, or assumes any legal liability or responsibility for the accuracy, completeness, or usefulness of any information, apparatus, product, or process disclosed, or represents that its use would not infringe privately owned rights. Reference herein to any specific commercial product, process, or service by trade name, trademark, manufacturer, or otherwise does not necessarily constitute or imply its endorsement, recommendation, or favoring by the United States Government or any agency thereof. The views and opinions of authors expressed herein do not necessarily state or reflect those of the United States Government or any agency thereof."

FINAL TECHNICAL REPORT

Thermoplastic Composites Parts Manufacturing Enabling High Volumes, Low Cost, Reduced Weight with Design Flexibility – Phase 1

Principal Investigator: Lee Silverman
Organization: E.I. DuPont de Nemours and Company, Inc.
Address: 200 Powder Mill Road, Building 323/227, Wilmington, DE
Phone: 302-695-4350
Email: lee.a.silverman@dupont.com

Co-authors:

Michael Bogdanor, Purdue University College of Engineering, Composites Manufacturing and Simulation Center, West Lafayette, Indiana, 47906
Robert Davies, Fibrtec Inc., Atlanta, Texas, 75551
Jacob Dickinson DuPont Company, DuPont Performance Materials, Wilmington, Delaware, 19803

Date Published:
April 2018

Prepared by
Institute for Advanced Composites
Manufacturing Innovation
Knoxville, Tennessee 37932
managed by
Collaborative Composite Solutions, Inc.
for the
US DEPARTMENT OF ENERGY
under contract DE- EE0006926

Project Period:
09/2016 – 04/2017

Approved for Public Release

List of Acronyms

CFRP	Continuous Fiber Reinforced Polymer
COM	Cost of Manufacture
IACMI	Institute for Advanced Composites Manufacturing Innovation
NNS	Near Net Shape
RFF	Rapid Fabric Formation
UD	Unidirectional

TABLE OF CONTENTS

ACKNOWLEDGEMENTS ix
EXECUTIVE SUMMARY 1
1.INTRODUCTION 2
2.TECHNICAL APPROACH AND RATIONALE 3
2.1 Technoeconomic Analysis 4
2.1.1 Competing composite processes 4
2.1.2 Reducing the Cost of the Intimate Carbon Fiber and Polymer Mixture 4
2.1.3 Reducing the Cost of Fabric Preform Production Using RFF 5
2.1.4 Reducing the Waste of Carbon Fiber using Near Net Shaping 6
2.2 Experiments, Modeling and Simulation of Draping in RFF Fabrics 6
3. RESULTS AND DISCUSSION 7
3.1 Technoeconomic Analysis 7
3.1.1 Model Assumptions 7
3.1.2 Analysis 8
3.2 Experiments, Modeling and Simulation of Draping in RFF Fabrics 10
3.2.1 Experimental Characterization 10
3.2.1.1 Unconsolidated Tow experiments 10
3.2.1.2 Optical Microscopy 11
3.2.1.3 DMA – Tension 11
3.2.1.4 DMA – Flexural 13
3.2.1.5 Unconsolidated RFF experiments 13
3.2.1.6 Picture Frame 13
3.2.1.7 Consolidated RFF Experiments 16
3.2.1.8 Unidirectional Plates 17
3.2.1.9 RF Plates 17
3.2.1.10 Microscopy 21
3.2.1.11 Unconsolidated RFF Model 21
3.2.1.12 Model overview 21
3.2.1.13 Model Inputs 23
3.2.1.14 Simulations of Shear Behavior 23
3.2.1.15 Uniaxial Tension Behavior 26
3.2.1.16 Using the Unit Cell in Manufacturing Simulations 26
3.2.1.17 Consolidated RFF Model 27
3.2.1.18 Model Overview 28
3.2.1.19 Consolidated RFF Model Inputs 30

3.2.1.20 Validation 31
3.2.1.21 Using the Unit Cell in Performance Simulations 31
4. BENEFITS ASSESSMENT 33
4.1 Commercialization Plan 33
4.2 Accomplishments 33
5. CONCLUSIONS 34
5.1 Recommendations 34
5.2 References 35
6. LEAD PARTNER BACKGROUND 36

LIST OF TABLES

Table 1. Geometric properties of the unconsolidated tows. 23
Table 2. Mechanical properties of the unconsolidated tows. 23
Table 3. Coated tow properties used in the consolidated RFF model. 31
Table 4. Effective composite properties of the consolidated RFF from the Unit Cell Model......................31

LIST OF FIGURES

Figure 1. Schematic of preform cross-sections showing a) UD tapes, b) fabric/film stacks, and c) coated tow. The polymer phase is blue, the carbon fibers are black, and voids are shown as white. 2
Figure 2. Rapid Fabric Formation laydown schematic...5
Figure 3. Potential routes to preform production...7
Figure 4. Cost of Manufacture (COM) of rectangular preforms from the three proposed routes..............8
Figure 5. Shape of the lower control arm demonstration part, provided by Ford, showing the use of RFF to produce a NNS preform 9
Figure 6. COM of manufacture (COM) of NNS preforms from the three proposed routes 9
Figure 7. Cross section of an unconsolidated tow 11
Figure 8. Tensile moduli of unconsolidated tows as a function of frequency 11
Figure 9. Measured flexural modulus is lower than measured tensile modulus 12
Figure 10. Picture frame test results for RFF and twill fabrics..13
Figure 11. RFF fabric in the picture frame fixture 13
Figure 12. RFF fabric at a very large shear angle..14
Figure 13. Bending stiffness measurement..15
Figure 14. Measured values of RFF fabric bending stiffness as well as the "average" of the measurements taken on each side...15
Figure 15. Stress-strain curves for pressed unidirectional samples. 16
Figure 16. Pressed and tabbed consolidated RFF...17
Figure 17. Consolidated RFF after surface grinding 17
Figure 18. Broken coupons 18
Figure 19. Stress-strain curve for consolidated RFF coupons...18
Figure 20. Surface strains of tensile coupons at about 1% average strain 19
Figure 21. Microscopy image of pressed RFF plate...20
Figure 22. Microscopy image of pressed RFF plate at a partial failure location 20
Figure 23. TexGen geometry of the unit cell consisting of 8 warp tows and 8 weft tows........................21
Figure 24. Abaqus finite element unit cell model of RFF 21
Figure 25. Twill unit cells generated by TexGen: (a) 2×2 and (b) 2×1. 23
Figure 26. Comparison of experimental vs. simulated response of shearing force to the shear angle of RFF fabric and 2x2 twill..23
Figure 27. Deformed unit cell of RFF at shear locking angle 24
Figure 28. Deformed unit cell of twill fabrics at shear locking angle: (a) 2x2; (b) 2x1 24
Figure 29. Uniaxial tension behavior of RFF and twill 2×1 and 2×2. 25
Figure 30. (a) PAM-FORM simulation of wrinkles induced in in RFF (left) and twill 2×2 fabric (right) with (b) contour plots of the distribution of shearing angle in RFF and twill 2×2 fabric.........................26
Figure 31. Multiple spatial scales of the composite from a) microstructure to b) RFF unit cell to c) structural component 27
Figure 32. Microstructure of the RFF a) Represented using TexGen and b) as seen in microscope images with c) a close up of an overlapping region 28
Figure 33. Consolidated RFF Unit Cell model for 8x8 0/90 configuration...28
Figure 34. Hex-packed composite micromodel for computing CT properties shown with von Mises stress. 29
Figure 35. Stiffness of the RFF unit cell with respect to shearing angle 31

ACKNOWLEDGEMENTS

The information, data, or work presented herein was funded in part by the Office of Energy Efficiency and Renewable Energy (EERE), U.S. Department of Energy, under Award Number DE-EE0006926 with the Institute for Advanced Composites Manufacturing Innovation (IACMI).

The authors would like to acknowledge the work of many team members that made this work possible, from project guidance, to administration, to execution. This extended and talented team included:

DuPont: Doug Anton, Janet Sawgle, Mary Strzlecky, Mark Weinberg, Bryan Sauer, Tao Huang, Tim Harper, Ryan Martin, Charles Woodward, and Zachary Dilworth.

Fibrtec: Penelope Salmons

Purdue: R. Byron Pipes, Tian Tang, and Nathan Sharp

IACMI: Dale Brosius, Lisa Fitzgerald, Erin Brophy, John Unser, and John Hopkins

Department of Energy: Kelly Visconti

Thank you all for your diligent and inspired efforts.

Executive Summary

In this project, a new carbon fiber composite manufacturing process has been demonstrated which has exhibited favorable fabric formability characteristics as compared to traditional woven materials. This new material combines Fibrtec's flexible coated tow, FibrFlex®, with DuPont's Rapid Fabric Formation (RFF) technology and a proprietary DuPont polyamide resin, all supported by Purdue University's extensive modeling and characterization capabilities. The coated tow material is a partially impregnated carbon fiber/polyamide composite tow where the carbon fiber is not fully wetted with the polyamide, yielding a more flexible tow material than one that is fully impregnated. The RFF process is an ultra-fast way of manufacturing fabrics with tows in varying orientations without the need to lift the tow during processing. Experiments, modeling, and simulations, all have shown that this process/materials combination is a potential method for producing lower cost continuous fiber reinforced polymer (CFRP) materials that conform well during molding with outstanding physical properties.

1. INTRODUCTION

Continuous carbon fiber composites can be divided into two broad classes based on their polymer matrix chemistries; thermosets and thermoplastics. Each material has its strengths, and the system that is chosen for a specific use depends on the detailed requirements of that particular application being considered. For example, thermoset composites are capable of Class A surfaces but have limited shelf life, require refrigeration, are not recyclable, and can require an extended time in the mold to take the polymerization process to the point where they are stiff enough to be unmolded. Thermoplastic composites, on the other hand, generally have rougher surfaces unless overmolded in a subsequent process step but can be thermally stamped in high rate processes relative to thermoset molding. In addition, thermoplastic stamping is a process that is reminiscent of the metal stamping process with which the automotive industry is quite comfortable.

Both composite systems have the unique combination of high strength and stiffness with low density, typical of continuous carbon fiber systems, which makes them ideal for reducing weight in vehicles, enabling among other things an increase in fuel efficiency. Their largest drawback, which is currently preventing wider commercial application, is a high cost relative to the weight saved. This high cost is due to both raw materials and fabrication. While the price of the carbon fiber itself is being addressed in separate IACMI projects, this program addresses other raw materials costs and the downstream fabrication cost of the composite parts.

There are several legacy manufacturing techniques for continuous carbon fiber based thermoplastic composite fabric preforms, again, each having its own strengths and weaknesses. The first technique is based on weaving dry carbon fiber tows into a fabric, layering these fabrics with thermoplastic resin films, and subsequently heating and compressing them into a well-consolidated composite (Figure 1b). One of the biggest costs with this technique is in the weaving of the carbon fiber tows. The stiff carbon fibers can easily break during weaving releasing short carbon fibers

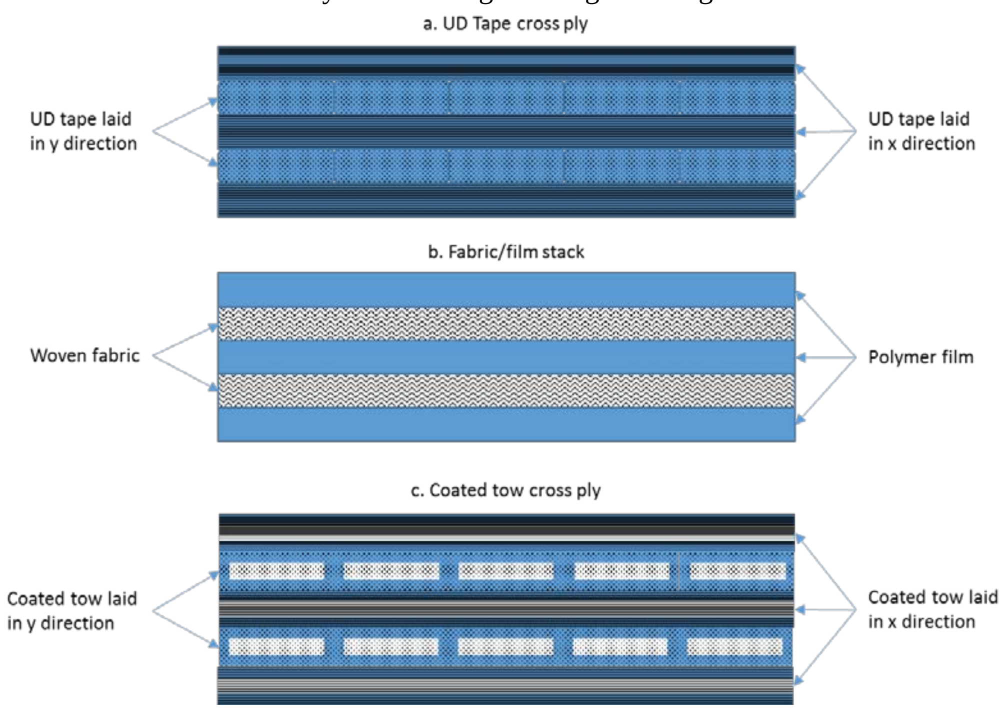

Figure 1. Schematic of preform cross-sections showing a) UD tapes, b) fabric/film stacks, and c) coated tow.
The polymer phase is blue, the carbon fibers are black, and voids are shown as white.

into the local environment. This conductive high aspect ratio debris can easily short out electrical equipment near the loom, and therefore the looms and nearby equipment need to be electrically isolated. Furthermore, the fiber properties also require that the looms be operated at relatively slow speeds, roughly one third the speed at which glass fiber-based fabric is made, adding additional capital related costs to the manufacturing process. This is also true for carbon fiber fabric co-woven with polymer filaments and combinations of woven carbon fiber and polymer powder. An additional potential drawback for processes based on woven fabric is their inability to conform to sharp corners and deep draws when molded. This occurs due to the "shear locking" of the fabric, leading to wrinkles and other fiber miss-orientation effects in the molded part.

Weaving processes also create rectangular fabrics from which the fabric layers required for the preforms must be cut. While this is acceptable for final composite parts that are substantially flat and rectangular in shape, it leads to significant trim waste when a non-rectangular part is desired. Since carbon fiber is the most expensive component of the fabricated composite part, the discarded expensive fabric is reflected in the high cost of manufacture of the finished composite.

Another general technique is the impregnation and flattening of the carbon fiber tows with a thermoplastic resin to make a low-void, fully consolidated composite tape (Figure 2a). These tapes are then woven or placed and tacked to form a fabric, which is then rapidly consolidated into the final composite part. A major issue with this process is the handling of the UD tapes because they are stiff and brittle, and therefore can fracture when bent to tight radii at room temperature. This stiffness property makes fabric formation from tapes a slow and expensive process.

The objective of this program was to reduce the cost of manufacture (COM) of carbon fiber CFRP composites by using a near net shape process (NNS) such as automated fiber placement (AFP) on a relatively inexpensive carbon fiber/polymer tow-preg. The coated tows are easily manipulated, and the resulting pseudo-fabrics are easily draped and conform easily during molding without shear locking. With this strategy, it should be able to use the expensive carbon fiber only where it is required, reduce the carbon fiber waste by up to 30%, and create fiber preforms that predictably deform during compression prior to molding.

In addition, the embodied energy was studied by Brosius and Deo[2]. The report summarizing the findings is presented separately and shows that the embodied energy was reduced by over 40 percent using this processing scheme.

The combination of these materials and process schemes will therefore lead to a decrease in cost for carbon fiber composite structures, making them more amenable for adoption in the automotive and other industries, reduce embodied energy, and directly lead to a creation of jobs in the industry.

2. TECHNICAL APPROACH AND RATIONALE

The project was performed in two major parts that were further subdivided. These were:

2.1 Technoeconomic impact

a. Competing composite processes
b. Reducing the cost of the intimate carbon fiber and polymer mixture
c. Reducing the cost of fabric preform production using RFF
d. Reducing waste of carbon fiber using Near Net Shaping

2.2 Experiments, modeling and simulation of draping in RFF fabrics

2.1 Technoeconomic Analysis

2.1.1 Competing composite processes

In order to understand how much the cost of continuous carbon fiber polymer composites could be reduced using the processes envisioned in this program, a technoeconomic analysis was performed and the results compared with competing technologies. In this step several composite making processes were compared on a cost basis at a high level. Since such analyses are highly dependent on the assumptions on which they are based, these are explicitly stated in the relevant section 2.1 of the results.

2.1.2 Reducing the Cost of the Intimate Carbon Fiber and Polymer Mixture

Regardless of the details of the CFRP processing rates for thermoplastic systems, CFRP production rates have historically been limited by the rate of intrusion of the polymer into the carbon tows due to the high inherent viscosity of the polymer matrix. The high viscosity is the result of the high molecular weights of the polymers required to attain the thermal and mechanical properties of the finished composites. The high viscosity of polymer combined with the small inter-fiber spaces characteristic of carbon fiber preforms through which flow is required typically results in extended hold times at temperature and pressure to achieve full or nearly-full consolidation. To reduce these extended hold times, this program used a proprietary DuPont polyamide thermoplastic polymer system with low viscosity. The result was a polyamide system that retained its mechanical properties and was useful at elevated temperatures.

Creating a fully consolidated composite from the fiber and polymer components is the crux of the composite- making process, all starting with a carbon fiber/polymer preform. There are many competing technologies for the production of thermoplastic composite carbon fiber preforms, each having a characteristic length scale associated with the distance over which the polymer must travel to produce a fully dense composite. On one end of this spectrum is fully impregnated void-free unidirectional tape, while the other end of the spectrum is represented by stacks of woven fabric interleaved with polymer film. Void free tape formation is very time intensive because the polymer is being driven into the fiber tows to eliminate porosity. The resulting tape is very stiff and does not conform well to molds at room temperature. Fabric/film layup formation is fast and inexpensive because there is no impregnation in the early part this process, and the drape of the fabric makes mold filling much easier.

The early process speed is compensated during the consolidation part of the process. In void-free UD tape, the polymer does not need to move very far for the part to achieve full density during consolidation, the tapes need only be bonded together, as shown in Figure 1a.. This makes the consolidation process fast. Conversely in the case of fabric/film stacks, the polymer must flow from the interlayer film all the way to the center of the woven fabric layer during consolidation, as shown in Figure 1b. The bottom line is that the time/temperature/pressure must be invested at some point during the composite forming process. This investment can be made at the beginning, as in tapes, or at the end, as in fabric/film stacks. By investing the time/temperature/pressure during the formation of UD tape, this process is inherently slower than the interleaving process. However, this investment is recouped during post-preforming consolidation, where tape can be thermally stamped to forge the final part. Interleaved materials must be either impregnated followed by stamping, or compression molded in order to consolidate the materials, and each of these processes require more time so as to allow polymer flow.

Alternatively, the tow coating process is faster than UD tape making, the tooling cost is lower, and it offers substantial automation potential making it ideal for mass production. The thermoplastic polymer/tow of choice for this project was Fibrflex® coated carbon tow. FibrFlex® is Fibrtec's core family of products. It is uniquely flexible and yarn-like, and it readily adapts to the shape of a mold, where in the presence of heat and pressure it is converted into a lightweight high strength part. The lower energy requirement coupled with being fully recyclable bolsters its recognition and value in the market. FibrFlex® can be produced at high rates, much faster than fully impregnated tapes, because full polymer impregnation is accomplished during a subsequent consolidation step that is done at high pressures.

FibrFlex® represents an intermediate case in the spectrum between fabric/film stacks and UD tapes. Because the tows are not completely impregnated, the tow coating process is fast and capital unintensive. As such, the production cost of FibrFlex® should fall between tapes and stacks. Because each tow is coated, the polymer needs to flow less distance during consolidation than interleaved fabrics and films, as shown in figure 1c. And as such, the consolidation times/costs should also be between tapes and stacks. In addition, because the coated tow is not completely impregnated, it is flexible and easily conform to molds. This gives FibrFlex the obvious advantage over fabric stack because FibrFlex® can be preformed to near-net shape in Advanced Fiber Placement machines and subsequently deep-draw molded, eliminating the large amount of potential waste generated when using fabric sheets. While some of the analysis has been completed and is presented here, the detailed technoeconomics of the consolidation part of the process are still in progress.

2.1.3 Reducing the Cost of Fabric Preform Production Using RFF

Carbon fiber weaving is slow relative to more flexible tow materials, and can lead to substantial fiber breakage, generating conductive dust that can subsequently work its way into nearby electrical components. In addition, near net shape preforms cannot be generated from woven fabrics. In this program, we used a lay down process patterned on DuPont patented Rapid Fabric Formation[1] (RFF). In this process the partially impregnated carbon fiber/polyamide composite tow (FibrFlex®) was particularly useful because it is very flexible. The RFF process is a means of manufacturing fabrics with tows or yarns in varying orientations without the need to lift the tow in the process. The laydown process is depicted in Figure 2. The layers of the fabric are held together in this material by locally melting the polyamide at the intersection between tows in specific locations to connect the top layer of tows to the bottom layer (black dots). This architecture has significant benefits over cross ply layups in that the bonded fabric is easily handled between laydown and molding, and that the tows should shift controllably during the molding process. As a result, it is believed, that it will have beneficial drape and conformability properties when inserted into a deep-draw compression mold, the type that may be typical for high stiffness structural parts.

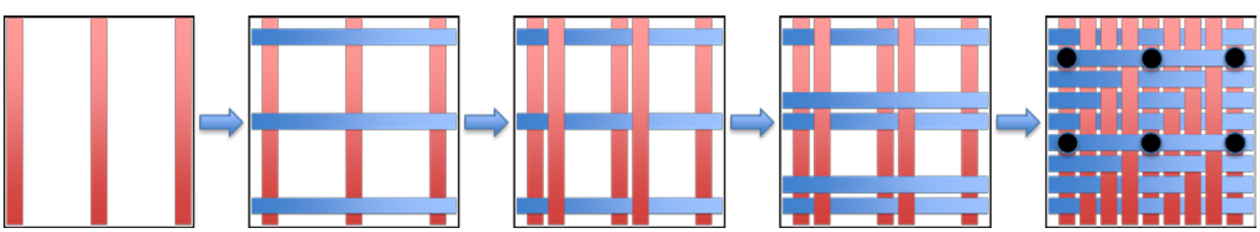

Figure 2. Rapid Fabric Formation laydown schematic.

The resulting fabric demonstrated a significantly lower resistance to shearing than a traditional woven fabric. This reduced the initiation of wrinkling in the preform during molding because wrinkling occurred at higher shearing angles than in the case of traditional woven materials. This in turn means that the manufacturing process can be applied to more complex geometries than have typically been possible with woven material systems.

2.1.4 Reducing the Waste of Carbon Fiber using Near Net Shaping

Carbon fiber is the most expensive material component in a CFRP composite, and as such, minimizing carbon fiber waste has a substantial impact on total costs. In traditional woven carbon cloth processes, wide rolls of cloth are woven, and appropriately sized and shaped pieces are subsequently cut out of the continuous web. This is exactly the process that has been used over the past two millennia to produce clothing and leads to roughly 30% of the initial material being wasted. To address this, we modified the RFF process (Figure 4 and Section 3.1 under Model Assumptions reflects the Preform Manufacturing Route 3) to include a near net shape component, akin to that used during automated fiber placement, which significantly reduced the amount of carbon fiber that is wasted during preform fabrication.

2.2 Experiments, Modeling and Simulation of Draping in RFF Fabrics

The development of a modeling and simulation strategy for utilizing this material/process combination is important in the present world of computer-aided design and computer-aided engineering. The modeling and simulation process included modeling the behavior of the coated tows, unconsolidated RFF fabric, the draping and forming process, the mechanical behavior of the consolidated composite, and the ultimate structural performance of the composite part. The simulation began at the scale of the coated tow to represent the flexural properties of the FibrFlex® tows accurately. The drapability of the unconsolidated RFF fabric is in turn dependent on the behavior of the coated tows and the topology of the RFF fabric, including the bond locations and cross over angles in the fabric. As such, the unit cell model for the RFF does not rely on additional characterization data performed at the fabric scale, but these experiments on the fabric are used to validate the simulated behavior of the fabric. This unit cell of the unconsolidated RFF provides the inputs for the draping and forming simulations that predict fiber orientation, fabric shearing angles, local mold pressures, and final part thickness. To predict the manufacturing-informed performance of the part after molding, a second unit cell model was exercised – that of the consolidated RFF material. Fiber orientation is critical for determining the local physical properties of the composite material that govern the residual stresses and deformation in the part coming off the molding tool and predicting the performance of the part. As the material rotates and shears, the mesostructure of the composite alters and, due to the anisotropy of the system, the physical properties change. This unit cell relies on mechanical testing of the tow material and constituent fiber and matrix. The fiber orientations and fabric shearing angles determined in a draping and forming simulation predict the local composite properties of the RFF, which in turn dictate the ultimate structural performance of the part.

3. RESULTS AND DISCUSSION

3.1 Technoeconomic Analysis

The scope of this analysis was to examine the cost of manufacture to produce unconsolidated near-net shape (NNS) preforms from the three routes shown in Figure 3.

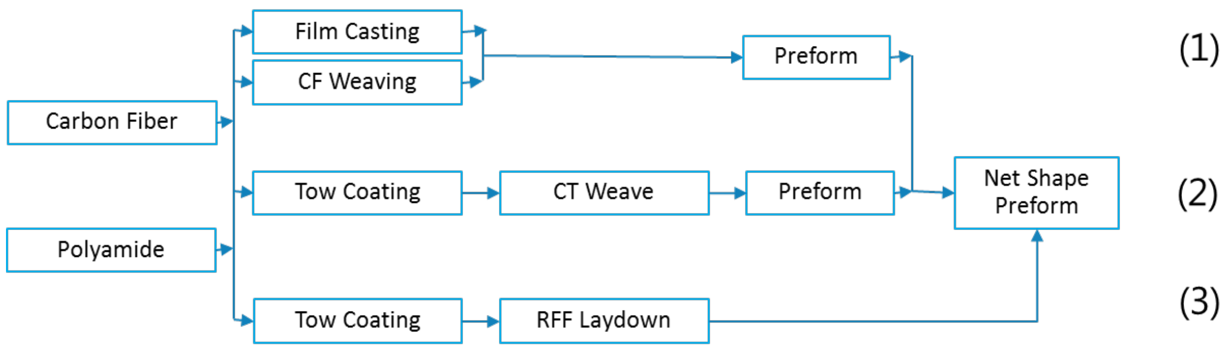

Figure 3. Potential routes to preform production

The analysis stopped at the NNS preform and did not consider the costs related to consolidation, part formation, trimming etc. These downstream processes, and the associated costs, will depend on the time/pressure/temperature required for full consolidation of the parts, especially when considering UD tape-based processes, and were not within the scope of this phase of the program.

3.1.1 Model Assumptions

The following assumptions were used to produce the techno-economic analysis. It is critical to note that the first two routes produce rectangular preforms due to the use of weaving. The proposed route which utilizes RFF, can directly produce NNS preforms with minimal waste.

Raw Material:

- 12k carbon fiber with appropriate sizing for PA = $9.50/lb
- Fully compounded DuPont PA resin = $2.05/lb
- Composites are 60 wt% fiber, 40 wt% resin

Preform Manufacturing Route 1: Film and Woven CF

- Film casting cost estimated from toll manufacturer (85% yield assumed)
- CF weaving cost estimated from toll manufacturer
- Cost of cutting NNS preform from rectangular preforms <u>not</u> estimated
- Recycle/reuse value of scrap PA and CF <u>not</u> considered

Preform Manufacturing Route 2: Tow coating and weaving

- High-volume (i.e., >2,000 metric tons/yr) coated tow production from Fibrtec
- 93% CF and 88% resin yield from tow coating process
- Coated tow weaving cost estimated from Fibrtec (98% yield assumed)
- Cost of cutting NNS preform from rectangular preforms <u>not</u> estimated

- Recycle/reuse value of scrap PA and CF not considered

Preform Manufacturing Route 3: Tow coating and RFF

- High-volume (i.e., >2,000 metric tons/yr) coated tow production from Fibrtec
- 93% CF and 88% resin yield from tow coating process
- Coated tow RFF cost estimated from proprietary DuPont machine design (98% yield assumed)
- Near net shape preform produced with 98% yield
- Recycle/reuse value of scrap PA and CF not considered

3.1.2 Analysis

The first section of this analysis examined the cost to produce a rectangular preform. These preforms can be produced with minimal waste from all three proposed routes. Figure 4 illustrates these costs assuming high-volume production (i.e., >2,000 metric tons/yr).

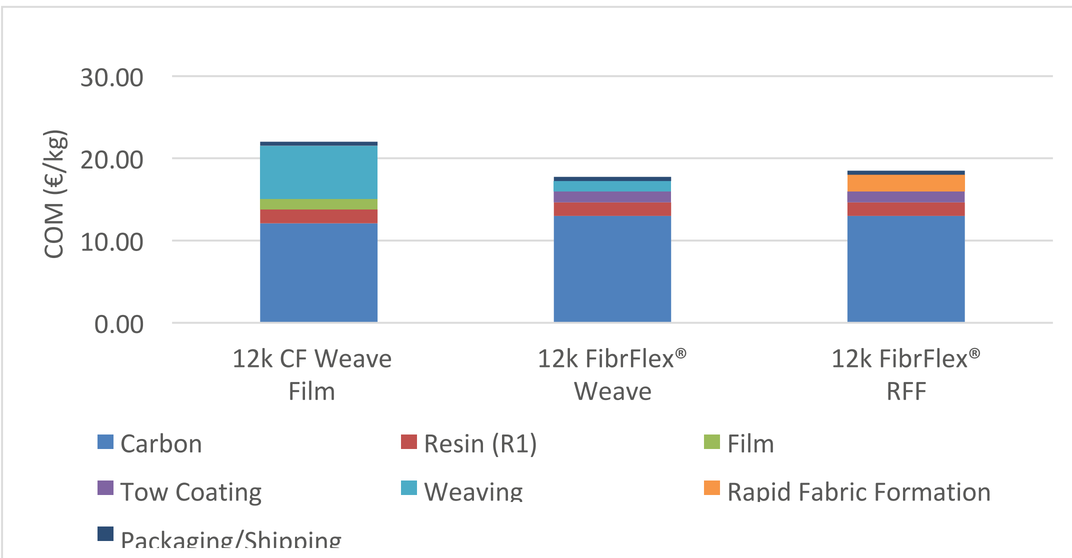

Figure 4. Cost of Manufacture (COM) of rectangular preforms from the three proposed routes.

Figure 4 shows that to produce rectangular preforms, the COM for the CT/weave route is essentially the same as the COM for the CT/RFF route. Both routes are cost-advantaged compared to the 12k CF/weave route. The key difference in cost between the latter two routes and the 12k CF/weave route is the cost associated with weaving 12k carbon fiber. It is our understanding that the cost for weaving CF is high due to the cost to isolate the looms to avoid electrical shorts from CF fibrils and the low rates of weaving CF due to its brittleness.

The second proposed route, CT/weave, reduces the COM to produce a rectangular preform by significantly reducing the weaving costs. The cost reductions are produced by first running the 12k CF tow through the tow-coating process and encapsulating the fiber in resin. As mentioned earlier in this report, the resulting coated tow, with the tradename FibrFlex®, is still flexible enough to be woven.

The CF is protected by the resin sheath, likely eliminating the need to isolate the looms and allowing for higher weaving rate. The weaving costs projected for this route were supplied by Fibrtec. During the course of this project, Fibrtec successfully demonstrated coated tow production rates greater than 130 feet per minute, substantially reducing the capital equipment that would be required to produce material for preform fabrication.

third proposed route, CT/RFF, has roughly the same estimated COM as the CT/weave route to produce rectangular preforms. A significant piece of the anticipated value of this manufacturing route is not captured in the simple analysis above to create a rectangular preform. To gain a better understanding the value of being able to directly create NNS preforms with minimal waste, it made sense to examine a proposed demonstration part. Working closely with an automotive OEM, we chose a lower control arm suspension component, based on its performance and dimensional requirements, to be used in Phase II of this program. Figure 5 shows this part.

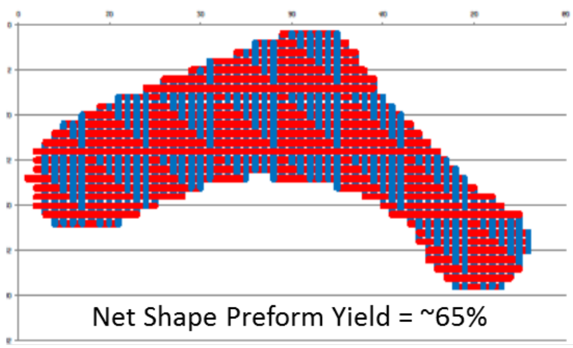

Figure 5. Shape of the lower control arm demonstration part, provided by Ford, showing the use of RFF to produce a NNS preform.

Simple nesting experiments of the proposed preforms, while maintaining the fiber orientation shown above, indicated that if the NNS preform was cut from a larger rectangular preform (i.e., analogous to routes 1 and 2 above), the yield of carbon fiber and resin into the preform would be approximately 65%. If we assume that a skilled composite engineer could find slightly more efficient methods to nest the desired part and assume a 75% yield for the first two routes and recalculate the COM for all three routes, we arrived at the figure shown below.

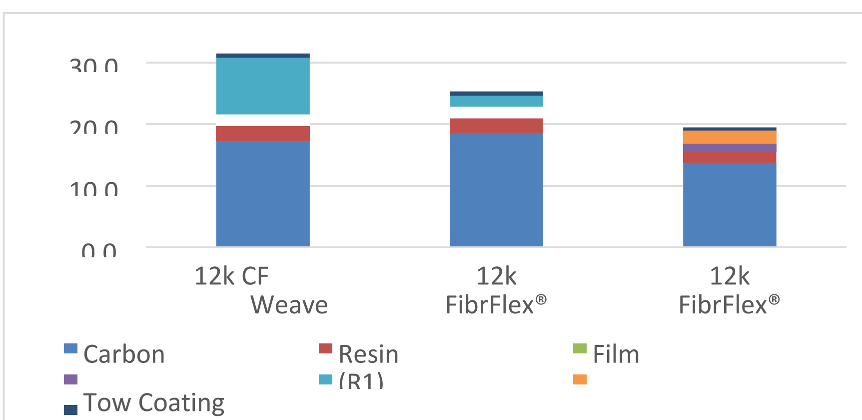

Figure 6. COM of manufacture (COM) of NNS preforms from the three proposed routes.

Figure 6 clearly demonstrates the value of the CT RFF route compared to the other two proposed routes due to the significantly lower COM. It is worth noting that the cost to produce these NNS preforms is driven largely by the cost of the carbon fiber. Therefore, maximizing the yield of carbon fiber from the bobbin to the final part is critical.

It is worth noting that NNS preforms can also be formed using other common composite preforming techniques. The other known technology is to cross ply UD tapes directly into a NNS preform. Using this manufacturing route would achieve the same COM reduction shown above, but the final preform would likely have inferior draping forming properties when compared the RFF material, especially for complex parts. A more complete analysis, which will require significantly more work, would also assign a value to the enhanced drapability and fiber alignment in the final part. Nonetheless, the simple analysis above indicated that the CT/RFF manufacturing route, with the listed assumptions, provides significant cost savings compared to the incumbent weaving-based routes.

Near net shape RFF drove the cost of preforms down further, because RFF is a very rapid laydown process that can be accomplished on inexpensive equipment that is suitable for traditional cross-ply fabrication, such as Dieffenbacher's Fiberforge process. This is possible because RFF relies on the laydown of parallel tapes or tows, with subsequent layers being applied at specific angles relative to the first to create a space filling layer. RFF will by definition be slower than a cross-ply structure made on the same machine. For instance, a full 0/90 cross-ply can be made in two passes. Due to the fabric design, a similar RFF fabric with an 8-tape unit cell will require 8 times as long, or 16 passes. Unless the laydown system is very fast, the process throughput loss may make the RFF system less cost effective.

This reduced laydown rate comes with the substantial benefit that the limited interlacing of the tows stabilizes the fabric, resulting is significantly less displacement of the fiber during consolidation. This feature, allowing the fibers to stay where they are required for the application, is well worth the laydown rate penalty discussed above.

Recent progress has been made in the area of tape laydown speed and equipment cost throughout the composites industry. For example, AZL (Aachen, Germany) is currently designing a machine that will lay down a full coverage single layer of tape in one second. If 8 double layers of material are required for a particular design, the full preform build will take 16 seconds. A similar build using RFF will take just over two minutes. This is considerably slower, but well within the requirements of a mass production market.

In addition, this purpose-built equipment will not require advanced robotics to create preforms as they are today. This will enable multiple laydown stations to be acquired for parallel process of preforms at less cost than the current generation of tape laydown machines, driving the cost of the resulting composites down even further.

3.2 Experiments, Modeling and Simulation of Draping in RFF Fabrics

3.2.1 Experimental Characterization

3.2.1.1 Unconsolidated Tow experiments

In order to populate a model of the unconsolidated RFF, the properties of the unconsolidated tow were characterized. The inputs were needed to generate the model are the tow modulus, fabric bending stiffness, and fabric tensile force as a function of shear angle. These properties do not have ASTM testing standards, but common methods for all measurements were used.

3.2.1.2 Optical Microscopy

Since the Fibrtec coated tows are not fully impregnated, an image of the coated tow microstructure was created to aid in modeling of the unconsolidated properties. Figure 7 shows a cross-section of an unconsolidated coated tow.

As the image shows, most of the tow has fibers that were free from resin in the interior. However, around the outside of the tow, there was a layer of neat resin that encapsulated the fiber. There were also with a few interior locations of very large pockets of neat resin. This microstructure led to a tow that was very flexible because the fibers are not load bearing. The width of the tow is 4.75 mm.

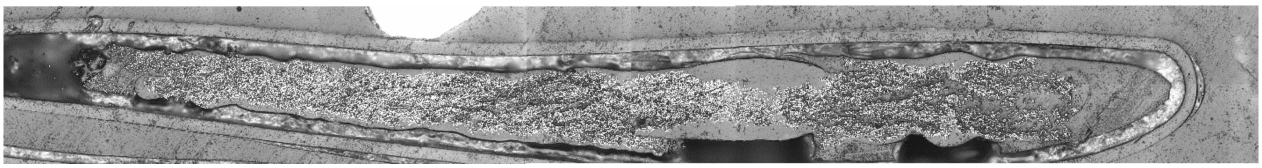

Figure 7. Cross section of an unconsolidated tow.

3.2.1.3 DMA – Tension

A dynamic mechanical analyzer (DMA) with a tension clamp was used to measure the tensile modulus of an unconsolidated tow. The DMA was utilized for this testing as the machine is designed to accept small material samples, on the same size scale of an individual coated tow and calibrated to be sensitive to loads at the order of magnitude required to precisely characterize the material. Seven samples were tested from a frequency range of 0.01 to 60 Hz. Figure 8 shows tensile storage modulus of the samples as a function of frequency along with the fixture used in the DMA to attain the measurements. As the figure shows, the tensile storage modulus ranged from 17 to 22 GPa with very little dependency on frequency. As the results indicated a negligible loss modulus, the tensile Young's modulus was taken to be equivalent to the storage modulus in this case. Based on the experimental results, it was decided to use 20 GPa as the tensile modulus input parameter for the unconsolidated RFF model. It was noted that the modulus of the unconsolidated tows was much lower than that measured in the consolidated specimens due to the large amount of voids in the unconsolidated material.

a) 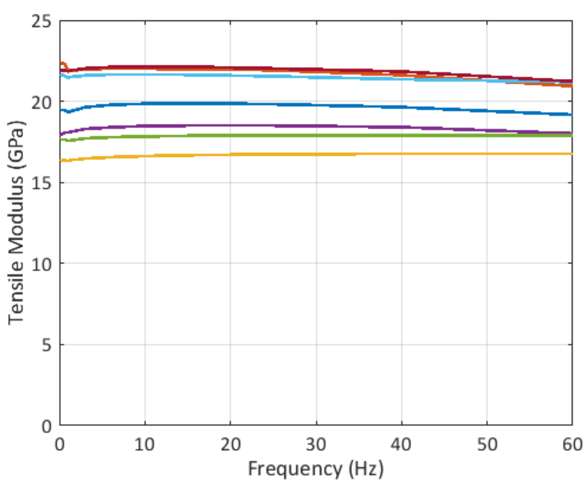

b) 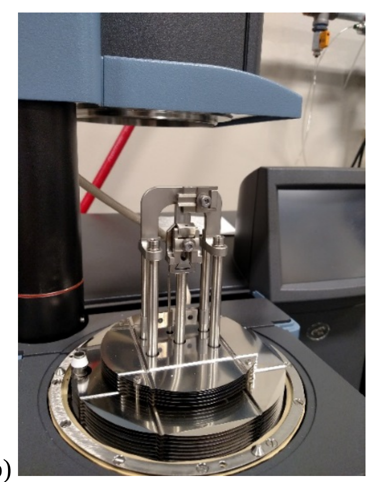

Figure 8. a) Tensile moduli of unconsolidated tows as a function of frequency from the b)

DMA with tensile fixture.

3.2.1.4 DMA – Flexural

The flexural modulus of the coated tows was also tested using a dual cantilever clamp on the DMA. Figure 9 shows the storage modulus computed from the flexural loading of an unconsolidated tow as a function of frequency. In this case, the modulus was measured as 13 GPa. Similar to the tensile tests, the negligible difference in storage modulus as a function of frequency indicated that the reported storage modulus from the dynamic test was equivalent to the elastic flexural modulus of the material. The discrepancy between tensile and flexural modulus was likely due to the fact that flexural modulus of the sample was highly weighted by the modulus at the outsides of the tow while tensile modulus was evenly weighted throughout the tow. Since the outside of the tows have large resin rich regions, this likely contributed to a decrease in the tow's measured modulus in flexure.

a) b)

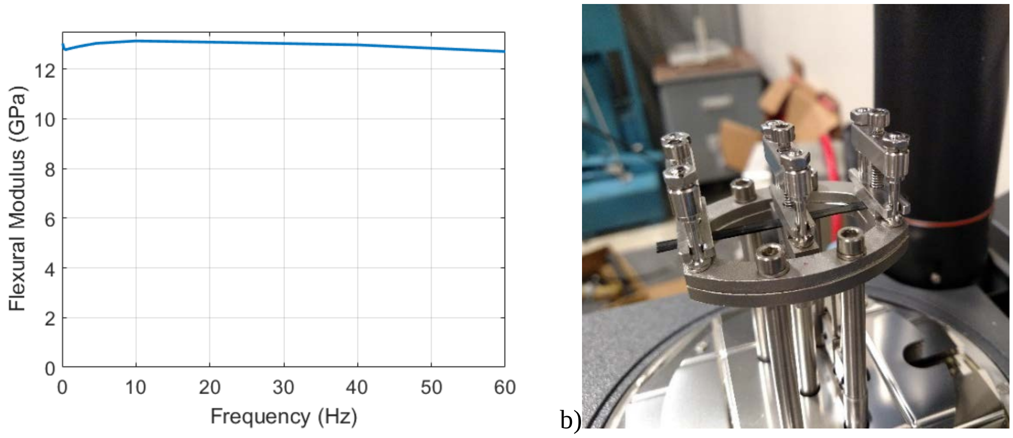

Figure 9. a) Measured flexural modulus from b) DMA with dual cantilever clamp fixture.

3.2.1.5 Unconsolidated RFF experiments

The unconsolidated RFF model also required having the bending stiffness properties of the fabric as well as the force required to shear the fabric, measured using a "picture frame" test.

3.2.1.6 Picture Frame

The unconsolidated RFF fabric was placed in a picture frame fixture and tested on a tensile testing machine in order to determine the force as a function of shear angle. In order to get a comparison point for the RFF fabric and a typical woven fabric, a twill fabric made from the same coated tows was also tested. Figure 10 shows the results of the picture frame test for the RFF and twill fabrics. Figure 11 shows the unconsolidated RFF in the picture frame fixture and Figure 12 shows the fixture at a very large shear angle (much higher than could be achieved in a woven fabric without wrinkling). As expected, the RFF requires much less force to shear than the carbon twill fabric and can shear farther before reaching the shear locking angle. In this case, the "shear locking angle" is taken to be at the intersection of the lines created by the two linear regions of the force vs. angle curves, and physically usually results in the occurrence of wrinkles and puckers in the fabric. In a woven fabric, this phenomenon occurs as a result of the woven tows being physically restrained from movement by the topology effects from the interlocked undulations of adjacent tows. In the RFF material, this topological interlocking does not exist, and "shear locking" in a traditional sense does not actually occur. The increase in slope of the force vs. angle curve around 40 degrees of shearing likely occurred due to slight imperfections in alignment of the tows in the fixture, e.g. tows not perfectly orthogonal to the mounting plates, and rotations near the ends of the tows resisting deformation.

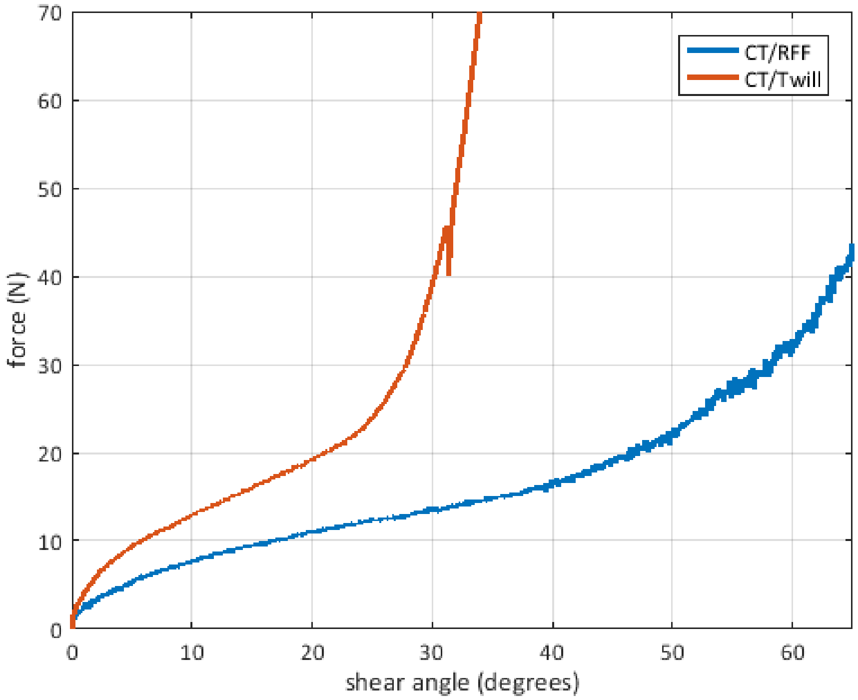

Figure 10. Picture frame test results for RFF and twill fabrics.

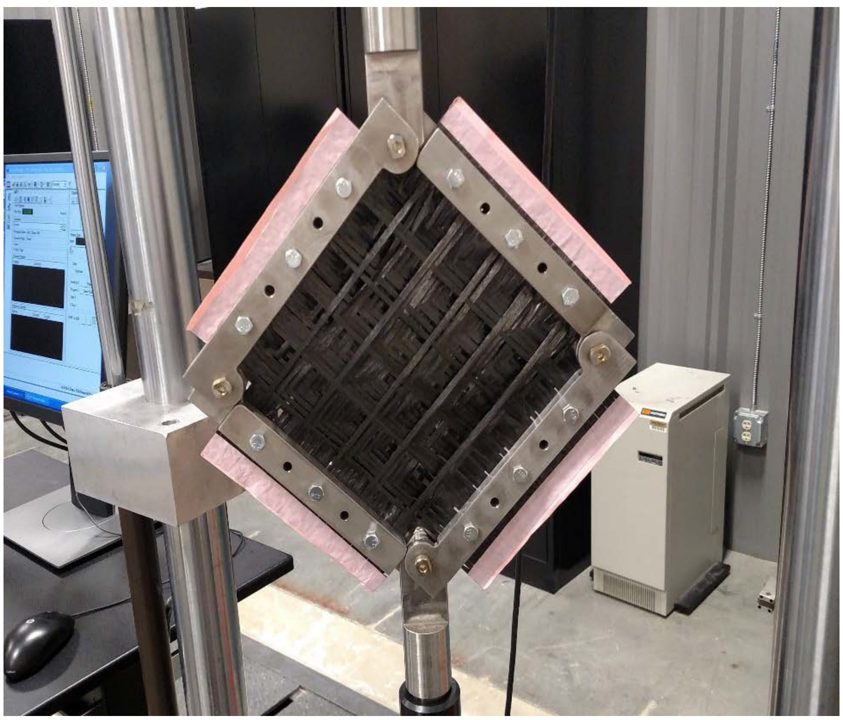

Figure 11. RFF fabric in the picture frame fixture.

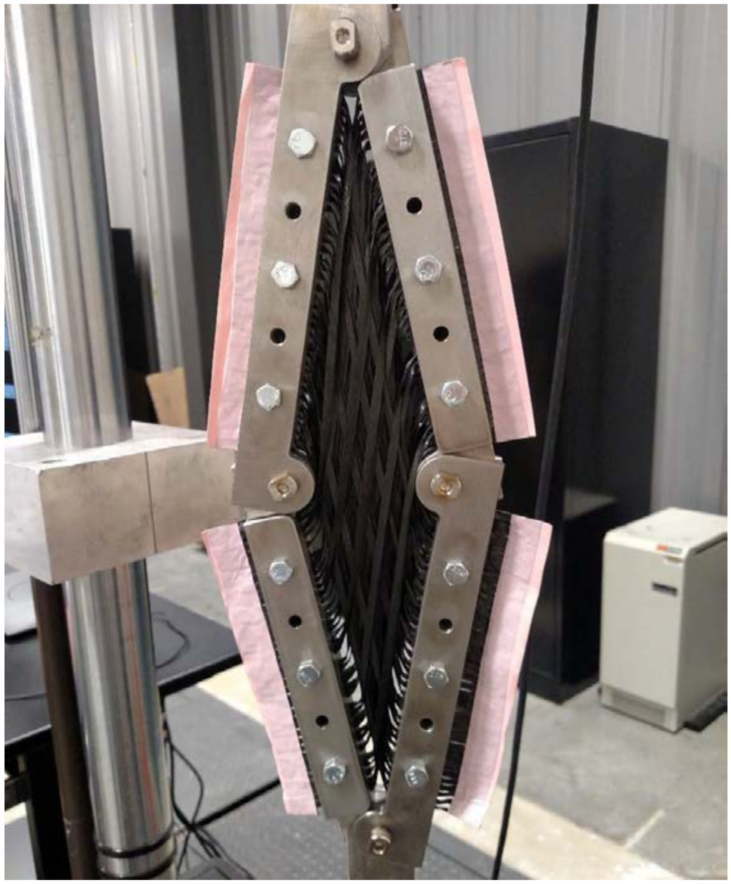

Figure 12. RFF fabric at a very large shear angle.

3.2.1.7 Fabric Bending

The bending stiffness of a fabric is typically measured by cutting a strip of fabric and hanging it over an inclined plane at a specific angle, increasing the amount of fabric that hangs over the edge until the end of the fabric touches the inclined plane. The bending stiffness is then backed out using beam equations. Measuring the fabric bending stiffness for the unconsolidated RFF fabric is difficult for a few different reasons. First, the fabric did not hold itself together. Therefore, tape had to be applied to the edges to prevent the fabric from falling apart. This may contribute to the bending stiffness, so the minimum amount of tape was used to mitigate the problem, but there is no way to eliminate it. Second, the test method was developed for fabrics with much lower stiffness and the fabric does not touch the inclined plane from bending under its own weight. A washer was taped to the fabric to increase the deflection. A modification of the equations was used to incorporate a point load at the end. A washer was not actually a point load, which incorporated another level of uncertainty to this measurement. The last problem was that the coated tows had some residual deformation to them, giving them a curvature in their stress-free state. This meant that the bending stiffness measurements were dependent on which side of the fabric was facing up. Three samples each were cut out of two different RFF fabrics and tested on the fabric bending stiffness tester. Figure 13 shows a fabric being tested and Figure 14 shows the bending stiffness results. Each fabric sample was tested on both sides and the lower and higher measured value are marked accordingly in the figure. As the figure shows, there is a lot of scatter in the data, but the average is consistent around 60 N/mm. Therefore, 60 N/mm was input as the bending stiffness into the model, although it should be noted that the actual measurements varied quite significantly from this value.

Figure 13. Bending stiffness measurement.

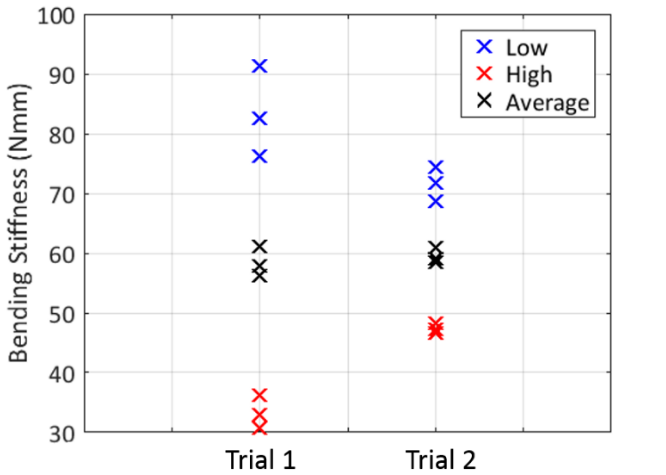

Figure 14. Measured values of RFF fabric bending stiffness as well as the "average" of the measurements taken on each side.

3.2.1.8 Consolidated RFF Experiments

A 10-inch square consolidated plate of unidirectional tows was pressed to measure the consolidated composite properties of the tows themselves. This plate consisted of a large number of unconsolidated tows that were aligned in a flat plate mold with closed walls and consolidated with 200 psi (14 bar) of pressure at 572°F (300°C) for five minutes. After this time, the mold was cooled while the pressure was maintained, and the tool opened after the plate cooled to under the glass transition temperature which is around 150°F (70°C). A 10 inch by 10-inch RFF plate was also pressed in order to validate the model which was created. This RFF plate consisted of four sheets of the 0/90 configuration RFF fabric with the 8x8 tow unit cell configuration. The plate was pressed in a similar process to the unidirectional plate, but 150psi (10bar) pressure was used and the walls of the flat plate were not in place for the pressing.

3.2.1.9 Unidirectional Plates

Seven one-inch wide tensile bars were cut from the unidirectional plates using a surface grinder and tested to failure in a tensile testing machine. The average thickness of the samples was 0.35 mm. The stress-strain results are shown in Figure 15. The samples showed tensile strength ranging from 1.2 to 1.5 GPa with an average modulus of 102 GPa.

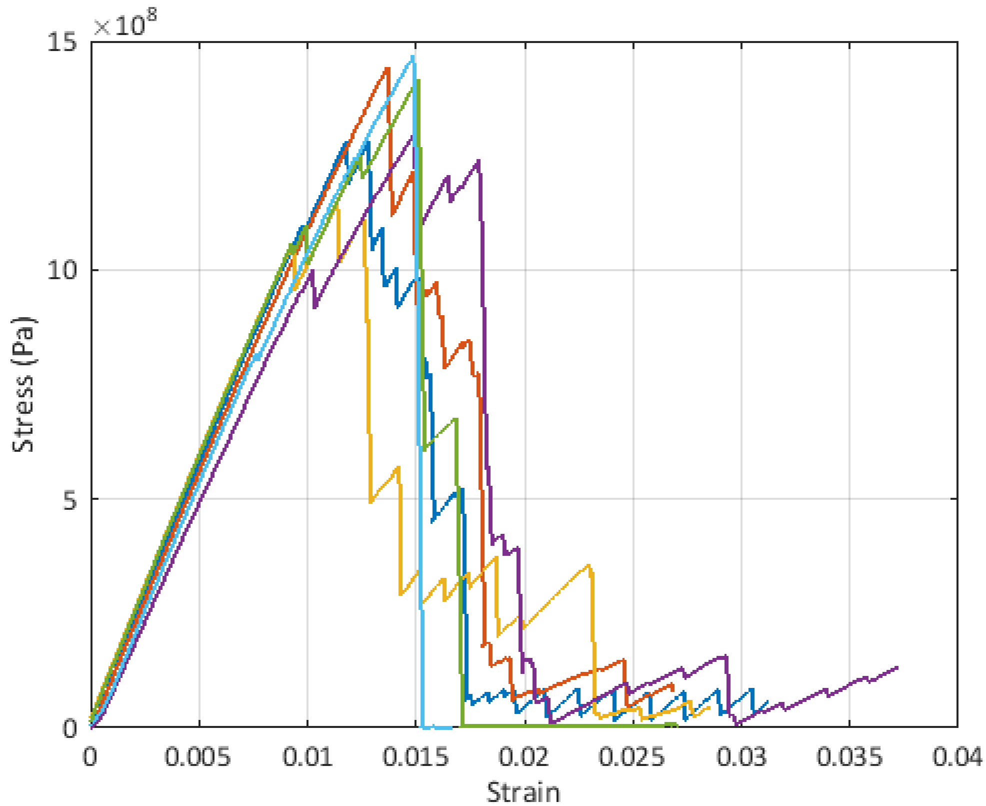

Figure 15. Stress-strain curves for pressed unidirectional samples.

3.2.1.10 RF Plates

RFF preforms using Fibrtec coated tows were provided to Purdue by DuPont and consolidated at 300 degrees Celsius and 150 psi pressure. The pressure was maintained until the temperature fell below the glass transition temperature of the polymer. The consolidated RFF plate was tabbed with fiberglass tabs and cut into 1-inch-wide coupons using a surface grinder. Figure 16 shows the coupons after being pressed and tabbed and Figure 17 shows the coupons after surface grinding. The coupons were speckled on one side which enabled DIC to be used to measure surface strain during the tests. The coupons were then pulled on a tensile testing machine to failure at 5 mm per minute. Figure 18 shows a photograph of the broken samples and Figure 19 shows the stress-strain curves of each of the samples. Based on the data shown in Figure 19, the average modulus of the consolidated RFF fabric is 54 GPa while the average strength is 741 MPa. These values are well above the minimum target values set for the program of 30 GPa and 300 MPa.

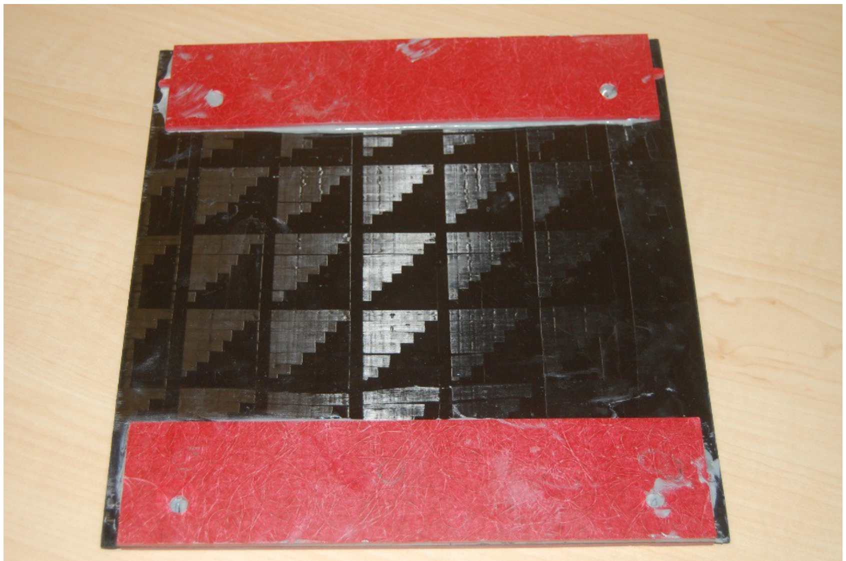

Figure 16. Pressed and tabbed consolidated RFF.

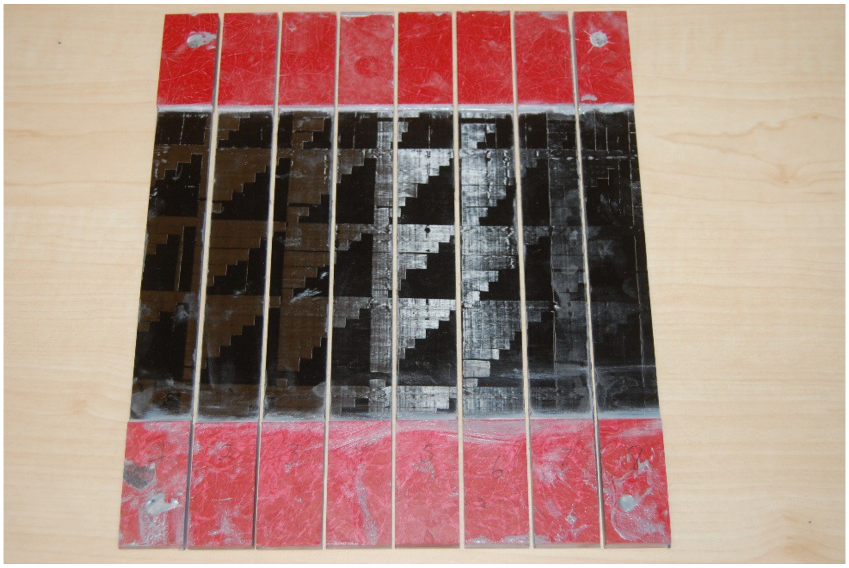

Figure 17. Consolidated RFF after surface grinding.

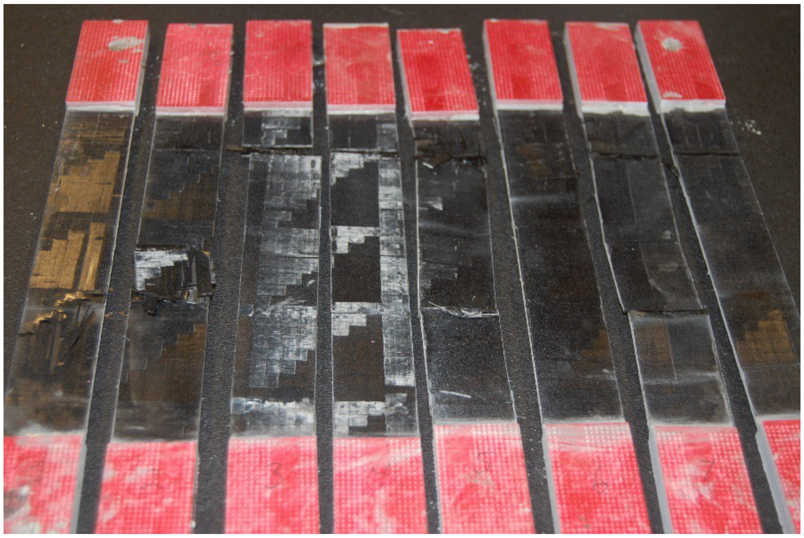

Figure 18. Broken coupons

.

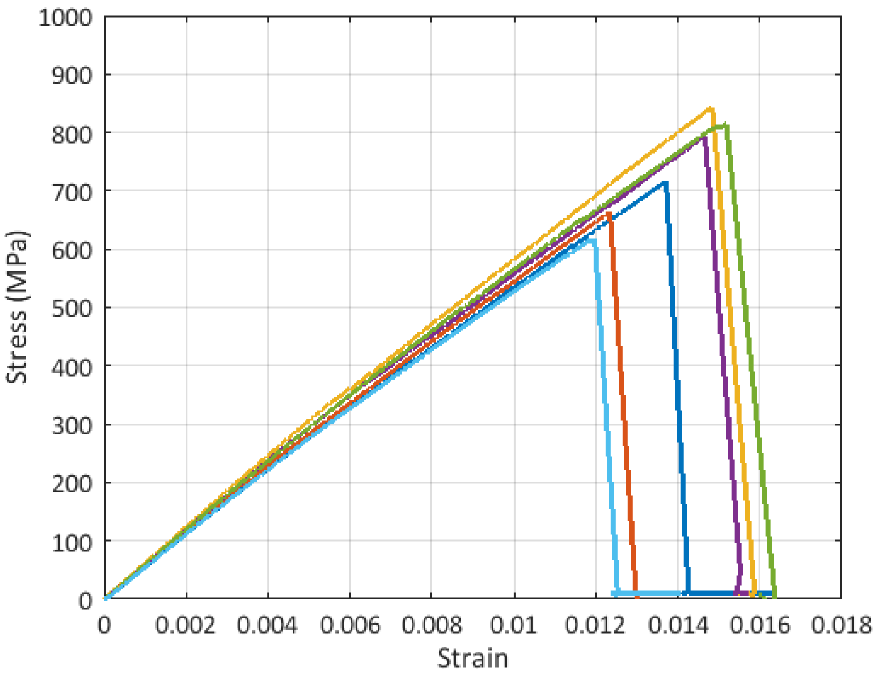

Figure 19. Stress-strain curve for consolidated RFF coupons.

Figure 20 shows a snapshot of the strains of each of the samples shown in Figure 19 from the DIC at about 1% strain on average. This shows that the surface strains are locally highest in regions of the fabric where the 90-degree tows are on the surface of the fabric. Every sample tested failed at one of these regions.

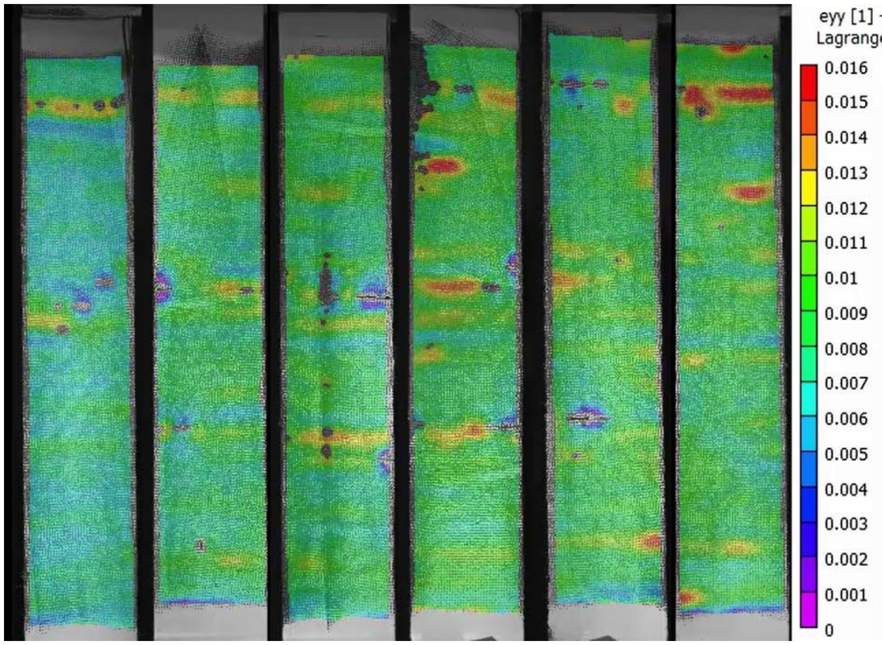

Figure 20. Surface strains of tensile coupons at about 1% average strain.

3.2.1.11 Microscopy

Microscope images were taken of the consolidated RFF fabric to validate the microstructure of the consolidated RFF model. Figure 21 shows a cross-section of one of the tensile coupons after being tested in a region that did not experience failure and Figure 22 shows a cross-section of a region that did experience failure (although not the primary failure location). As the figures show, the different layers wave quite a bit throughout the plate.

Figure 21. Microscopy image of pressed RFF plate.

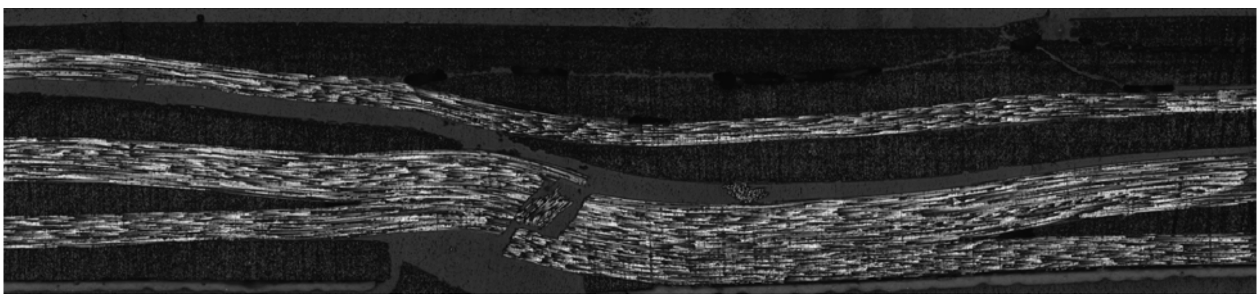

Figure 22. Microscopy image of pressed RFF plate at a partial failure location.

3.2.1.12 Unconsolidated RFF Model

The drapability and forming behavior of a composite fabric is governed by the mechanical interaction between the yarns or tows that make up the fabric. The purpose of the unconsolidated fabric unit cell model is to predict the draping and forming behavior of the fabric based on its material and topological construction. The coated tow in the RFF manufacturing process presents a yarn material that is different than traditional woven products. As such, it is imperative to incorporate the physical properties of the coated tow in the unit cell model of the RFF fabric. In addition to the difference in the tow, the RFF process results in a fabric structure that is very different from the product of woven processes. The lack of geometrical interlocking and the presence of bonds between tows produced by the local melting and cooling of the matrix material present unique features for the fabric unit cell.

3.2.1.13 Model overview

The open source software TexGen was employed to create the unit cell of RFF as shown in Figure 23. The generation methodology of the unit cell was implemented into Python input files of TexGen. The tow path is represented by the tow center line in three-dimensional space, which is generally a polynomial spline. The cross section of each tow formed by cutting the tow with a plane perpendicular to the tow path tangent was modeled as power ellipse in this study. The geometry of the tow was actually generated by sweeping the cross section along the tow path. The geometry of the RFF was imported into Abaqus to generate the finite element unit cell model as shown in Figure 24. The thickness, tow spacing, and tow width of the unit cell are listed in Table 1. The geometric and mechanical properties of both weft and warp tows of RFF are identical.

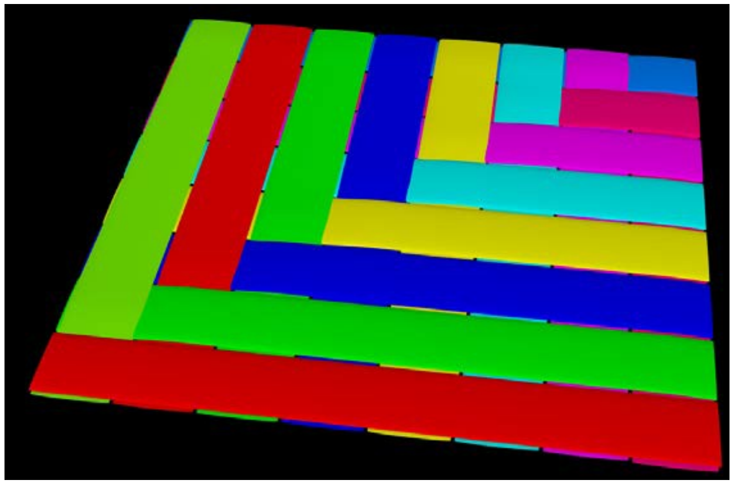

Figure 23. TexGen geometry of the unit cell consisting of 8 warp tows and 8 weft tows.

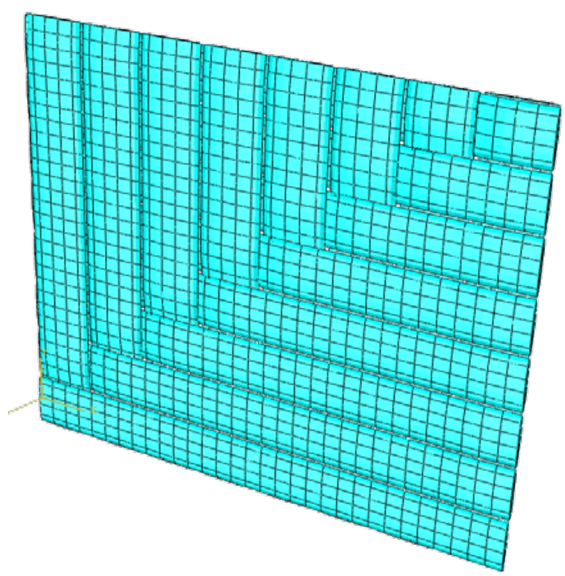

Figure 24. Abaqus finite element unit cell model of RFF.

Table 1. Geometric properties of the unconsolidated tows.

Tow spacing (mm)	Tow width (mm)	Fabric thickness (mm)
4.6	4.4	0.5

The fabric is assumed to be composed of numerous periodic unit cells to which the periodic boundary conditions are applied to replicate their periodic nature. The periodic boundary conditions were implemented into a python script. Since the woven fabrics were considered as two-dimensional continuum in plane stress state during forming process, the periodic boundary conditions were applied to the unit cell in two dimension as well.

The contacts between the tows were modeled using surface-to-surface technique with finite sliding. The normal behavior of the contact was chosen as "Hard" contact. The friction between objects follow the Coulomb's friction law, namely, $T_s = \mu T_n$ with T_s and T_n being the friction force and normal force, respectively. The coefficient of friction used between the tows in the models was measured experimentally at DuPont and determined to be 0.2.

The tows undergo large rigid body rotation and small local strain during shear deformation of the dry woven fabrics. It is critical that the material orientations of the tows are properly defined and rotate as the tows rotate during shear deformation. The rotation of material orientations can be achieved by turning ABAQUS NLgeom (geometrical nonlinear solver for large displacements and deformations) on in Step setting. The basic idea is to rotate the local material coordinate system through a rotation matrix extracted from the deformation gradient.

3.2.1.14 Model Inputs

The axial modulus of the tows is much larger than the transverse modulus and shear modulus. Since the dry fibers inside the tows are capable of sliding, the results is a low longitudinal shear modulus and low bending stiffness of the tows. However, the resin coated surface layer might increase the longitudinal shear modulus and the bending stiffness. The tows are orthotropic materials whose material properties are presented in Table 2.

Table 2. Mechanical properties of the unconsolidated tows.

E_{11} (MPa)	$E_{22} = E_{33}$ (MPa)	$G_{12} = G_{13}$ (MPa)	G_{23} (MPa)	υ_{12}	υ_{13}	υ_{23}
20,000	800	100	333.33	0.2	0.2	0.2

3.2.1.15 Simulations of Shear Behavior

For comparison, we also developed finite element unit cell models for Twill 2×1 and 2×2 fabrics using the coated tows. Figure 25 shows the geometries of twill 2×1 and 2×2-unit cells created by TexGen.

Figure 26 illustrates the variations of shear stress with respect to the shear angle for RFF and the 2x2 twill fabrics. This figure also compares the simulation result to the picture frame experimental data, showing good agreement between the experiments and the simulations. It is evident that the RFF fabric was much less resistant to shearing than the twill fabric or similar woven fabrics. It is inferred from this behavior that the RFF will also exhibit superior drapability. Figure 27 and Figure 28 show the deformed unit cells of RFF and twill 2×1 and 2×2 at shear locking angles. The RFF fabric did not exhibit a true "locking" phenomenon up to 45 degrees but did exhibit some confinement effects after 45 degrees of adjacent tows touching whilst not mechanically interlocking. The twill weaves, however, demonstrated mechanical interlocking closer to 20 to 30 degrees.

a)

b)

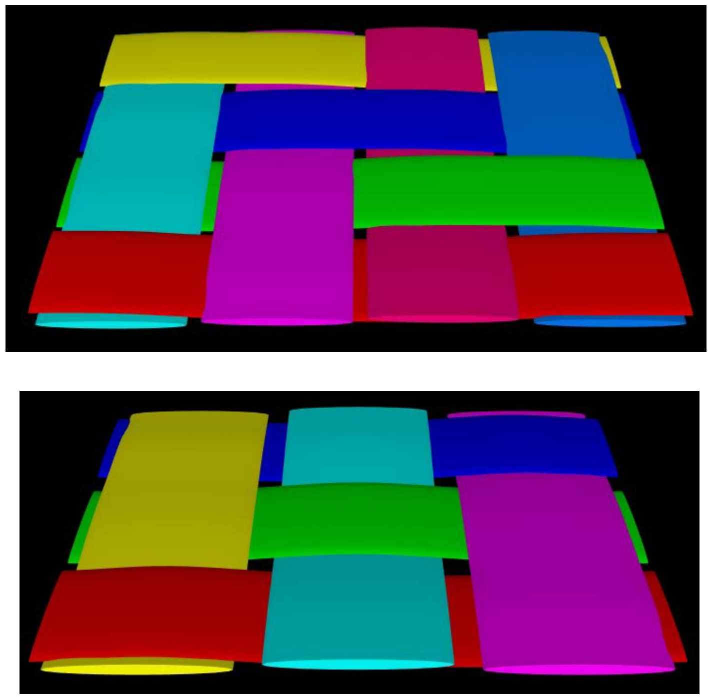

Figure 25. Twill unit cells generated by TexGen: (a) 2×2 and (b) 2×1.

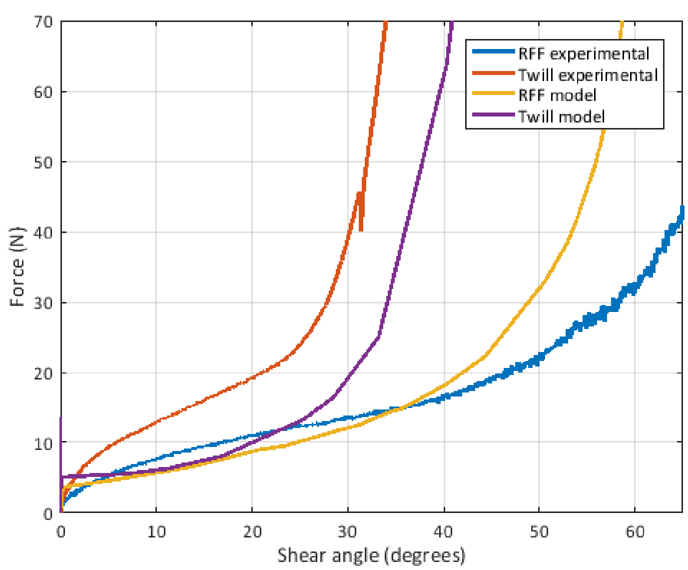

Figure 26. Comparison of experimental vs. simulated response of shearing force to the shear angle of RFF fabric and 2x2 twill.

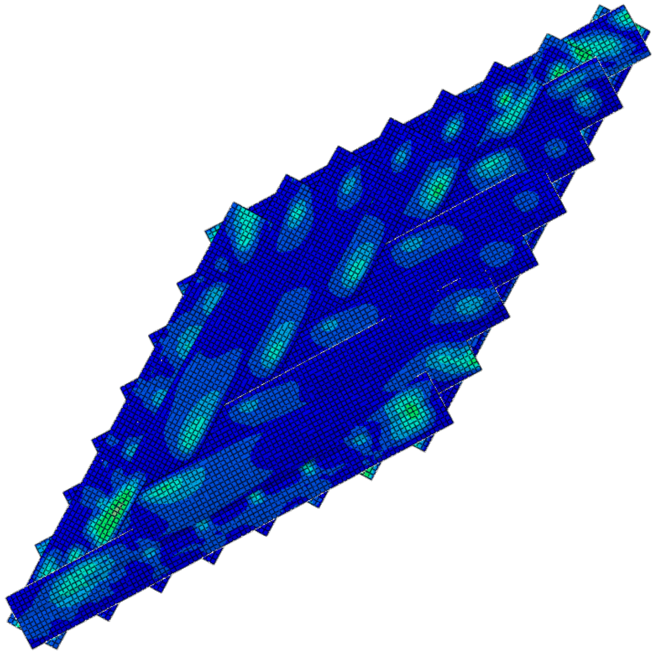

Figure 27. Deformed unit cell of RFF at shear locking angle.

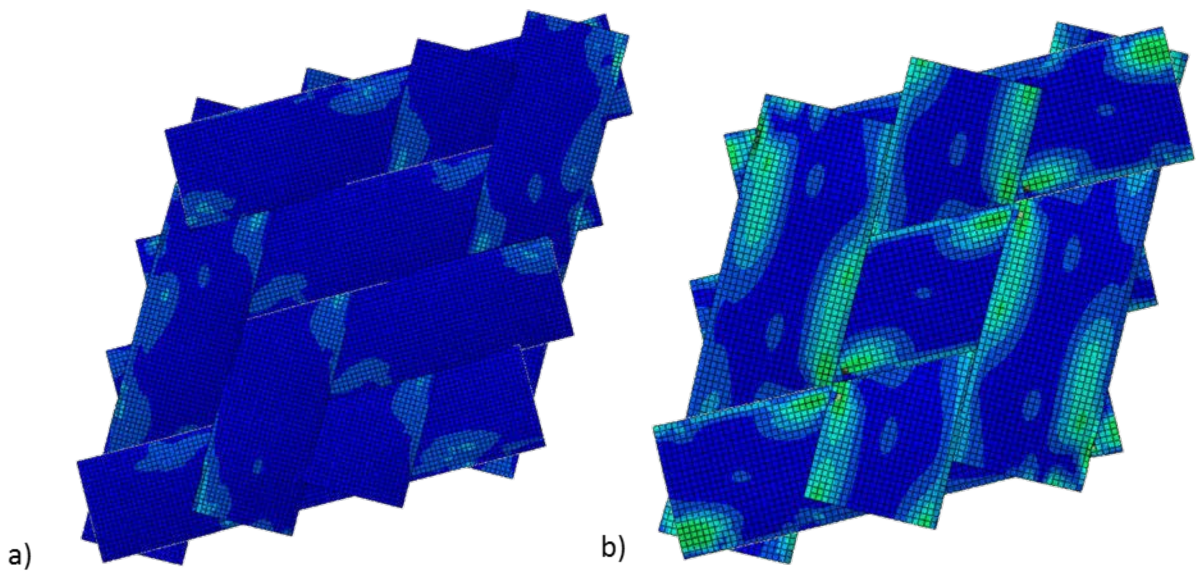

Figure 28. Deformed unit cell of twill fabrics at shear locking angle: (a) 2x2; (b) 2x1

3.2.1.16 Uniaxial Tension Behavior

Figure 29 presents the uniaxial stress-strain curves of RFF, twill 2x1, and twill 2x2 fabrics. The RFF has stiffer tensile behavior than that of twill 2x1 and 2x2 because the lack of crimps of the yarns of RFF results in stronger tensile response. The twill 2x1 exhibits the weakest tensile behavior due to its highest crimp of the yarns.

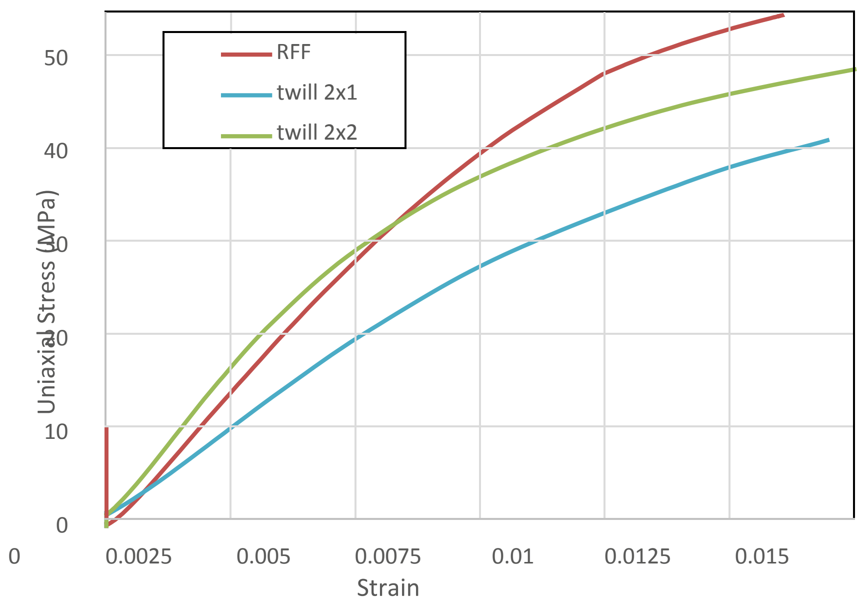

Figure 29. Uniaxial tension behavior of RFF and twill 2×1 and 2×2.

3.2.1.17 Using the Unit Cell in Manufacturing Simulations

The unconsolidated unit cell model described in this section provided a method for generating the input parameters for forming simulations based on the tow properties and fabric topology. Therefore, with the tows characterized, designers are free to explore the effects of changing the fabric topology on forming behavior. The accurately characterized fabric model reduced the amount of experimental iterations required in making and testing different fabric forms. To evaluate a different RFF configuration, the engineer will modify the inputs to the unconsolidated RFF model, analyze the shear locking, bending, and tensile behavior of the resulting fabric, and use that as the input values for the draping and forming simulation. In order to demonstrate the influences of material properties of RFF and Twill 2×2 fabrics, PAM-FORM, a commercially available composites forming simulation software was deployed to simulate the forming process of the RFF and twill 2×2 fabrics as shown in Figure 30. The size of the two fabrics are identical and formed into two identical adjacent square cavities. It is observed that there are more wrinkles generated in the twill 2×2 fabric than in RFF.

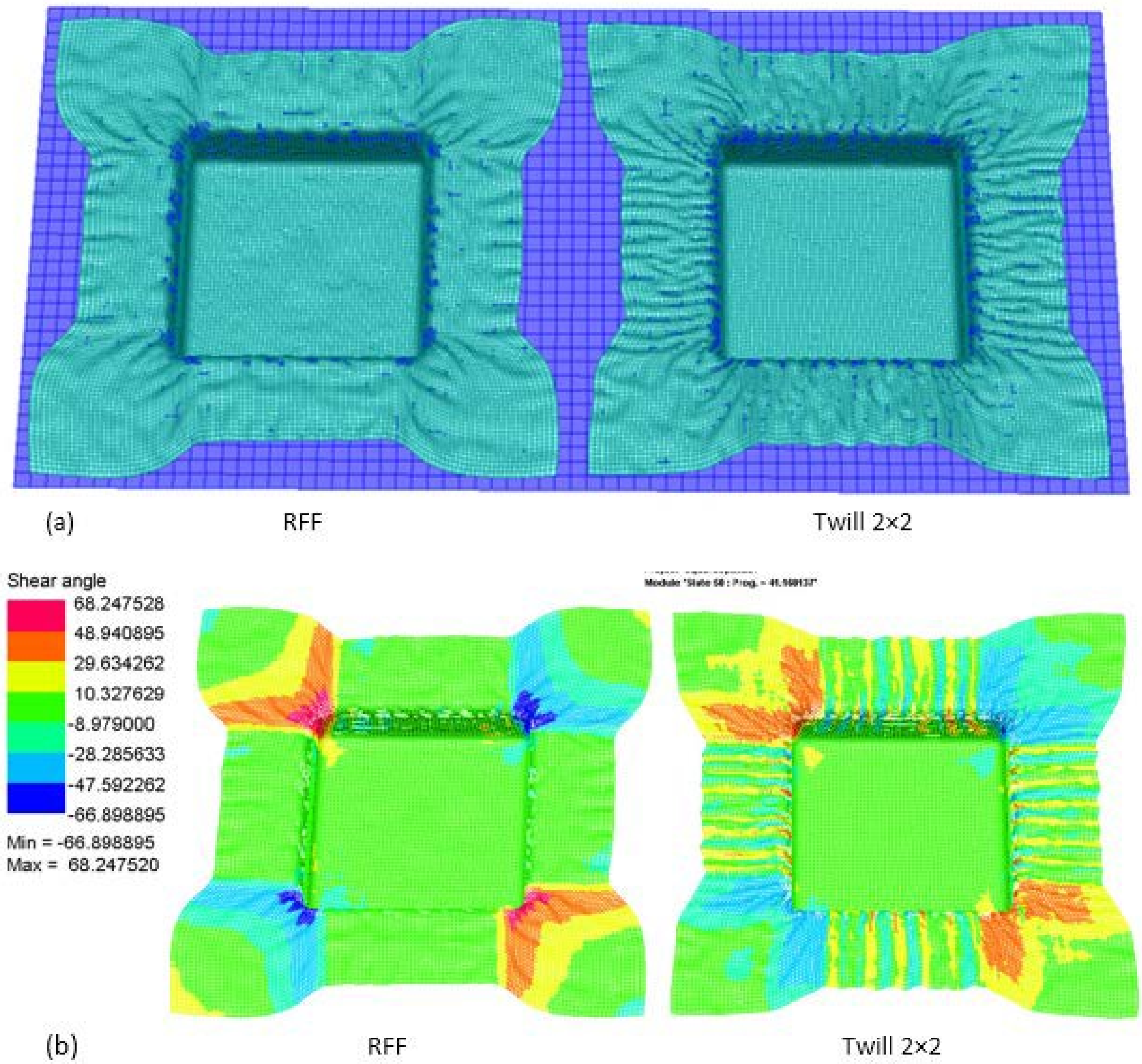

Figure 30. (a) PAM-FORM simulation of wrinkles induced in in RFF (left) and twill 2×2 fabric (right) with (b) contour plots of the distribution of shearing angle in RFF and twill 2×2 fabric.

3.2.1.18 Consolidated RFF Model

In order to utilize the internal fabric topology information obtained using the unconsolidated RFF unit cell in the draping and forming simulations, a robust model for the behavior of the consolidated RFF material is required. In this section, the unit cell for the consolidated RFF material is described which is constructed from the constituent material properties of the tows and the micro-topology of the pressed material. The initial models are constructed for the nominal alignment of the tows in a 0/90 configuration, but consideration is also given for modifying the unit cell to represent the changes in composite properties that are expected as the fabric shears and deforms.

3.2.1.19 Model Overview

Multiscale homogenization is an analysis tool for components and structures where material properties, structural topology, and response fields of interest are present at widely varying spatial scales. Figure 31 shows this multiscale framework in the case of a part made from the RFF manufacturing process. At the smallest scale, the microstructure of the tows is comprised of the continuous carbon fiber reinforcement and the polyamide resin. These two materials have significantly different mechanical properties, but at larger scale, even going up to the unit cell of the RFF fabric, this heterogeneity is not observable. In the RFF fabric, the topology and anisotropy of the individual tows produces different mechanical properties depending on the orientation of the tows and the presence of undulations where tows cross over one another. This meso-scale behavior is homogenized again to yield the properties of the composites material at the scale of a structural component. The properties at the structural scale, or the macroscale, are critical to the design of the component from a traditional part design standpoint, but additional material and manufacturing parameters are present at the micro- and mesoscales that are critical for accurate prediction of the performance of the part. These parameters are modified by design in the case of the fiber volume fraction, materials used, or the topology of the RFF, or altered in manufacturing such as when fibers change orientation during draping and forming. In both cases, it is important to understand these effects through a robust modeling approach.

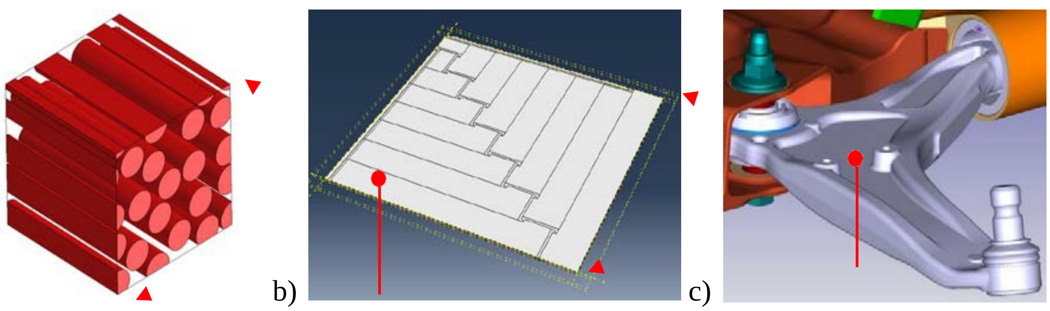
a) b) c)

Figure 31. Multiple spatial scales of the composite from a) microstructure to b) RFF unit cell to c) structural component.

Microstructural models that yield the homogenized properties of the fiber and matrix unit cell shown in Figure 30a have been well established. Commercial software such as SwiftComp, Digimat, Abaqus, and others provide industry-standard predictions for this scale of modeling. While unit cell models for traditional woven fabrics have been supported by software packages such as TexGen, the particular topology produced from the RFF manufacturing process is not supported by available codes specifically. The key difference is that in traditional woven microstructure, significant resin-rich pockets exist due to the interlocking undulations of the fiber tows, the required in-plane separation between tows to achieve a non-intersecting geometry, and the tows are represented by ellipses.

The TexGen representation of the cross-section of an 8x8 geometry of the fabric is shown in Figure 32a. Compared to the microscope image of this cross section in Figure 32b, the topology constructed from the fabric geometry generation shows distinct gaps at the boundaries of adjacent tows that are not visible in the physical system. In addition, the consolidated RFF geometry shows that the tows deform significantly at the location where the perpendicular tow changes its plane. These geometrical features affect the mechanical behavior of the unit cell and can contribute to stress concentrations and failure initiation locations in the composite material.

a)

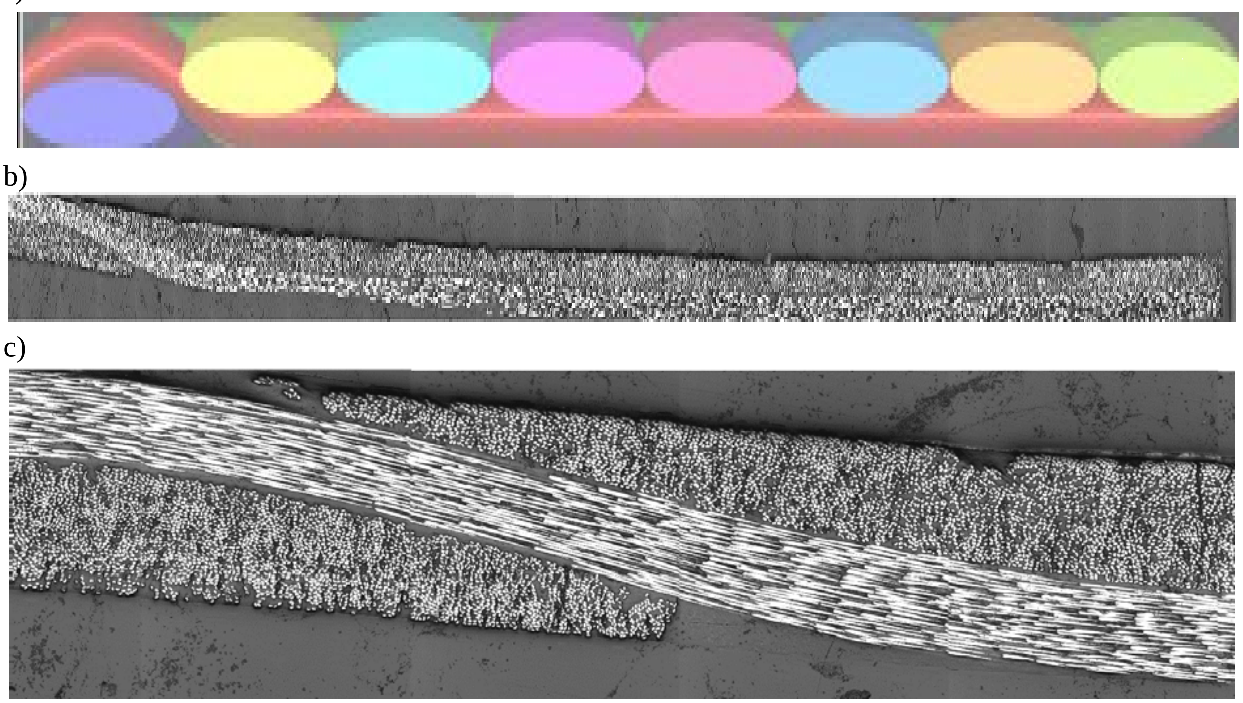

Figure 32. Microstructure of the RFF a) Represented using TexGen and b) as seen in microscope images with c) a close up of an overlapping region.

The model for a consolidated RFF unit cell with eight tows in either direction oriented in a 0/90 configuration is shown in Figure 33, as modeled in Abaqus. The geometry for this Unit Cell was constructed using python input scripting in Abaqus to create a framework for generating a variety of Unit Cell constructions varying the tow dimensions, number of tows, and tow lay-down order. The relative orientation of the tows can also be changed by modifying the geometry of this unit cell. The key features of this model are that the adjacent tows are touching, and the overlaps seen in Figure 31c are captured in the geometry. Periodic boundary conditions were employed in this model to minimize boundary effects on the effective homogenized properties. The model was analyzed for six loading cases representing the three normal strain states and three shear strain states. The volume average stress over the unit cell was then used to compute the elastic stiffness matrix for the unit cell. The nine engineering constants representing the orthotropic material were then computed from this 6x6 stiffness matrix.

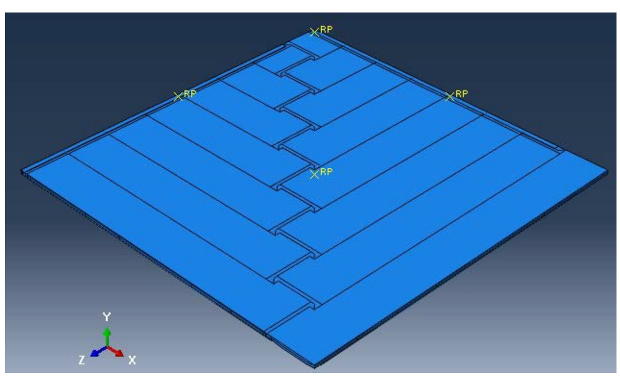

Figure 33. Consolidated RFF Unit Cell model for 8x8 0/90 configuration.

3.2.1.20 Consolidated RFF Model Inputs

The inputs for the consolidated RFF model included both geometrical inputs and physical property inputs. The geometry of the tows was taken directly from the microscope images in Figure 31b, c and using digital calipers. For the 56% fiber volume fraction tows provided by DuPont and Fibrtec, the average width of a single tow was 4.32mm and average thickness was 0.202mm. From the microscope images, the transition between planes for a tow occurred at a 7° angle from the horizontal, which was used to model the undulation of the tow in this region.

In this phase, the primary physical property investigated was the elastic stiffness of the composite. The stiffness of the composite material is predominantly governed by the longitudinal stiffness of the carbon fiber. In the unit cell model for the RFF fabric the individual coated tows are modeled transversely isotropic materials defined by five material properties: E_1, E_2, ν_{12}, ν_{23}, and G_{12}. The longitudinal modulus, E_1, was measured from the tensile experiments performed on the unidirectional coupons manufactured from the coated tows and reported as 1020 MPa.

The four remaining properties, E_2, ν_{12}, ν_{23}, and G_{12}, were not measured experimentally in this study but were computed using a micromechanical model of a hex-packed unit cell of the composite, as seen in Figure 34. The inputs for the micro-model were the transversely isotropic elastic properties of the carbon fiber itself, the isotropic elastic properties of the polyamide matrix, and the fiber volume fraction. In this study, a fiber volume fraction of 56% was reported from Fibrtec.

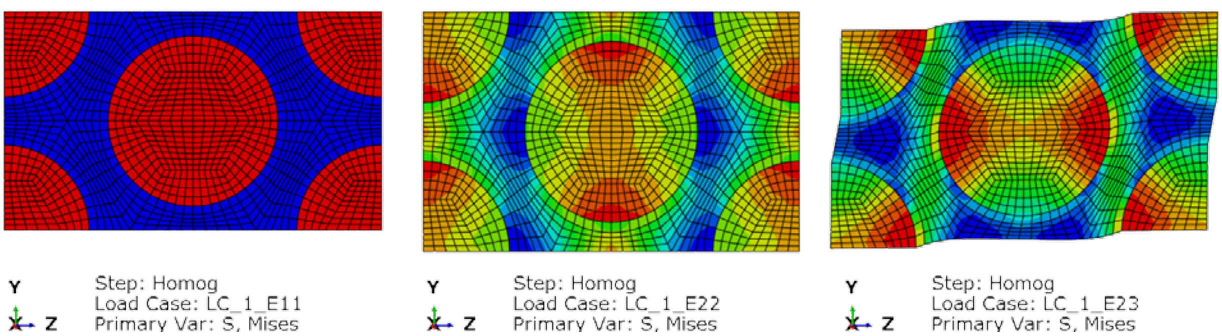

Figure 34. Hex-packed composite micromodel for computing CT properties shown with von Mises stress.

The mechanical properties for the fiber and matrix were selected from material data sheets. The polyamide was taken to have a Young's modulus of 2 GPa and Poisson ratio of 0.4. For the carbon fiber, only the longitudinal modulus of 240 GPa was reported. Assumed values for the remaining four inputs were taken to be E_{2f} = 17 GPa, ν_{12f} = 0.3, ν_{23f} = 0.3, and G_{12f} = 18 GPa, based on prior experience working with carbon fibers. It is noted that the transverse and shear moduli of the carbon fiber are significantly lower (less than 10% of) the longitudinal modulus of the fiber. The resulting composite properties from the microstructure analysis were E_{1f} = 135 GPa, E_{2f} = 5.3 GPa, ν_{12f} = 0.283, ν_{23f} = 0.492, and G_{12f} = 2.2 GPa. The longitudinal and shear properties are primarily governed by the matrix material while the fiber governs the longitudinal properties. It is noted that the computed longitudinal stiffness was significantly greater than the value observed in the experiments. This could have been due to incorrect processing parameters in making the coupons, fiber/tow misalignment resulting in orientation deviation, incomplete consolidation, variations in fiber volume fraction from the reported value, or fiber damage in processing and handling. Regardless of the source of the variance, the lower measured value for longitudinal stiffness was used in the RFF model. A sensitivity study was performed on these values with E_{2f} = [13,21] GPa, ν_{12f} = [0.2,04], ν_{23f} = [0.2,04], and G_{12f} = [12,24] GPa, which resulted in no variation in the longitudinal stiffness of the composite microstructure and a range of transverse stiffness between 5.3 GPa and 6.1 GPa, indicating that these fiber parameters have a minor effect on the homogenized composite properties. The final material properties used to represent the coated tow are shown in Table 3.

Table 3. Coated tow properties used in the consolidated RFF model.

Property	**Value**
Longitudinal Modulus, E_1	102 GPa
Transverse Modulus, E_2	5.3 GPa
In-plane Poisson ratio, ν_{12}	0.283
Transverse Poisson ratio, ν_{23}	0.492
Shear Modulus, G_{12}	2.2 GPa

3.2.1.21 Validation

The RFF unit cell model was analyzed for its effective composite properties using Abaqus. The resulting engineering constants are shown in Table 4. The measured longitudinal stiffness of the consolidated RFF material from experiments was 54 GPa, which is in very good agreement with the stiffness value predicted from the unit cell model.

*Table 4. Effective composite properties of the consolidate*d RFF from the Unit Cell Model.

Property	Value	Property	Value	Property	Value
E1	51.4 GPa	ν_{12}	0.445	G_{12}	8.4 GPa
E2	6.1 GPa	ν_{13}	0.03	G_{13}	8.7 GPa
E3	51.6 GPa	ν_{23}	0.05	G_{23}	8.4 GPa

3.2.1.22 Using the Unit Cell in Performance Simulations

One of the key benefits of using multiscale methods to predict the material properties of composites for use in simulation is the ability to predict all of the components of the anisotropic stiffness matrices for the composite. Experimental methods for out-of-plane properties in particular rely on complex test procedures that can become prohibitively expensive, especially when multiple material forms are considered. Furthermore, this unit cell is able to react to changes in the shearing angle of the fabric and provide predictions for the mechanical properties of the sheared fabric based on the physical behavior of the system. The shearing angle of the fabric has a significant effect on the mechanical properties of the fabric, as seen in Figure 35. In stress analyses for actual parts, the consolidated RFF unit cell model will be tied to the outputs from the forming simulation to provide oriented material properties throughout the part based on the shearing angle of the fabric at each integration point location. This results in a performance analysis that is informed by the manufacturing process.

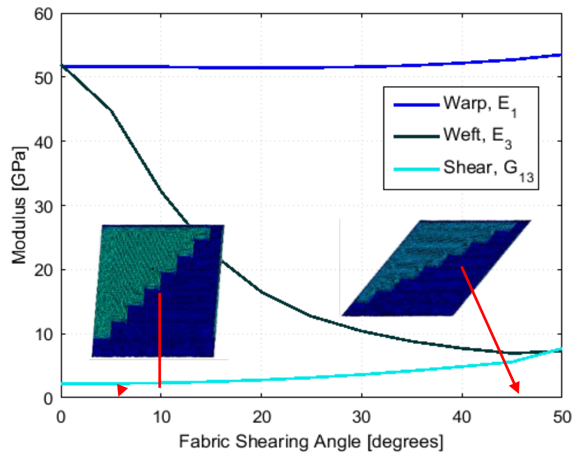

Figure 35. Stiffness of the RFF unit cell with respect to shearing angle.

4. BENEFITS ASSESSMENT

The results of the work described above demonstrates that the cost of manufacture of continuous carbon fiber composites can be significantly reduced by employing a near-net-shape Rapid Fabric Formation process using FibrFlex® coated tow technology. In addition, enhanced drape of FibrFlex® fabrics made using coated tow materials in RFF, as well as enhanced control of fiber motion during molding allows more complex shape formation. With these benefits, relatively inexpensive complex CFRP composites should be enabled, with cycle times and costs low enough to allow penetration into mass market applications. Reduced COM of carbon fiber composite parts will enable faster market penetration in to high volume commercial applications. This will drive energy savings through system lightweighting and associated support for job creation in the composites industry.

As stated on the IACMI website:

"IACMI's research, development, and demonstration programs will be driven by major industry participation with a focus on reducing technical risk and developing a robust supply chain to support a growing advanced composites industry."

This program has been focused on the fabrication and characterization of RFF-based parts and has de-risked the adoption of relatively low cost CFRP composites based on RFF technology for mass market industries.

Also stated on the IACMI website

"The Institute for Advanced Composites Manufacturing Innovation, IACMI, is committed to delivering a public-private partnership to increase domestic production capacity, grow manufacturing and create jobs across the US composite industry."

Through substantial cost reduction of thermoplastic composites, this project has the potential to broaden the domestic industrial manufacturing base for these products, with the follow-on impact of creating high quality jobs.

4.1 Commercialization Plan

These results have shown that the cost of continuous carbon fiber composites can be reduced by using Fibrtec's coated tow technology combined with near net shape processes such as automated fiber placement. This will lead to accelerated adoption of these materials into mid-range value applications such as those in the automotive industry.

4.2 Accomplishments

This project has shown that coated-tow technology combined with automated fiber placement will lead to reduced cost of carbon fiber composite. In addition, these materials have been shown to have beneficial draping properties that will allow enhanced conformation to mold shapes.

5. CONCLUSIONS

Phase I of this program was completed at the end of March 2017. During this phase of the program, a significant de-risking of the technology was demonstrated.

First, a preliminary technoeconomic forecast was created that compared the processing costs of the CT/RFF technology to existing composite manufacturing methods. The analysis indicated that CT/RFF technology will enable creation of preforms at a 30% savings relative to existing dry carbon weave/PA film consolidation technology. A major portion of the benefit comes from the ability of CT/RFF to directly make near net shape preforms, eliminating the majority of the carbon fiber waste.

Second, a process was developed to produce coated tow at greater than 100 feet per minutes. The process speed is currently limited by the uptake equipment rather than by the coated tow formation process. This limitation is easily overcome by making straight forward mechanical modifications to the winder to maintain the 130fpm speed.

Third, a production for making RFF fabrics was demonstrated with variable crossover angles and variable bonding density. Specifically, fabrics with 0/90 and 60/120 orientations were made with different bonding programs

Fourth, consolidated RFF fabrics were strength tested. The produced data indicates that stiffness and strength of the consolidated RFF CFRP composites are greater than 90% of the theoretical maximum for 0/90 laminates.

Fifth, one commercially viable part that can benefit from this technology was selected for evaluation in future work. Ford worked with the Team to assess multiple applications. As a result, a lower control arm was selected as a commercially viable target.

Finally, models were developed for the deformation of unconsolidated RFF fabrics and the mechanical properties of the consolidated composites. These models predicted that there will be a substantial benefit in fabric draping for molding RFF materials when compared to 2,2 twill carbon fabrics.

5.1 Recommendations

In Phase 2 of this program, we will apply these learnings to the production of Ford Fusion lower control arms so that the concepts can be demonstrated in an industrially relevant application, and the reduced COM of CFRP parts can be proven out. In order to prove this out, there are several steps that need to be demonstrated.

First, the manufacture of the coated tow needs to be reproduced. The results from Phase 1 were encouraging and going forward we need to show that these results are the rule rather than the exception.

Second, the mechanical property data from plaques created from coated tow needs to be gathered along with Ford's mechanical requirements for input to simulation models to create the detailed lower control arm design. This detailed design must include not only the shape of the finished part, but also the orientation and placement of the individual carbon fiber tows required to provide the strength and stiffness of the finished part.

Third, automated fiber placement must be demonstrated to create RFF fabric panels, and subsequent to the production of the detailed design, AFP will be used to create the fabric preforms required for the production of the actual lower control arm parts.

Fourth, the fabric preforms must be consolidated using compression molding to create dense parts for testing.

Fifth, the finished parts that result from consolidation must be tested in Ford's lower suspension test apparatus to ensure that they meet the Ford's design criteria. Finally, a cost model must be created for a process capable of rapidly creating RFF fabric preforms.

The program, as outlined above, will provide the data required for determining if the process for making carbon fiber composite parts using coated-tows and AFP will be amenable to cost low moderate performance parts, for industrial applications such as the automotive industry.

5.2 References

1. Popper, P., Walker, C.W., Tam, A.S., Yngve, P.W., Odle, J.K., and Thomson, G.Y, Rapid Fabric Forming, US Patent 6,107, 220
2. Brosius, D. and Deo, R., Impact of Technology Developments on Cost and Embodied Energy of Advanced Polymer Composite Components, IACMI Final Report, in press.

6. LEAD PARTNER BACKGROUND

DuPont is a worldwide science company dedicated to solving challenging global problems, while creating measurable and meaningful value for its customers, employees and shareholders. Our dynamic portfolio of products, materials and services meets the ever-changing market needs of diverse industries in more than 90 countries. We unite around a set of core values—safety and health, environmental stewardship, highest ethical behavior and respect for people—just as we have for two centuries.

Because innovative products such as CFRP are useful throughout many industries, we are focused on developing innovative solutions where the unique properties of strength, stiffness, and density give these materials a cost-effective performance advantage over incumbents.

As such, carbon fiber composites will be one part of a vast array of our offerings to the automotive industry, because choosing the right material is crucial to balancing the need to design low-emission, fuel-efficient vehicles without compromising performance, comfort and cost. With more than 100 high-performance product families and technologies and a global network of development experts, DuPont helps the automotive industry deliver efficient vehicles and elevate the driving experience.